April 2015

Calibration of an Intermediate Scale Fire Test Rig for Exterior Wall Assemblies: Source Fire

Blake Joseph Cornachini
Worcester Polytechnic Institute

Matthew Wheelock Foley
Worcester Polytechnic Institute

Scott Sheppard Knight
Worcester Polytechnic Institute

Thomas John Ritchey
Worcester Polytechnic Institute

Calibration of an Intermediate Scale Fire Test Rig for Exterior Wall Assemblies: Source Fire

A Major Qualifying Project Report

Submitted to the Faculty of

WORCESTER POLYTECHNIC INSTITUTE

In partial fulfillment of the requirements for the

Degree of Bachelor of Science by:

Blake Cornachini (ME)

Matt Foley (CE)

Scott Knight (ME)

Tom Ritchey (ME)

Date: April 30, 2015

Approved:

Professor Nicholas Dembsey, Major Advisor

Authorship Page

Section	Author(s)
1. Introduction	Foley
2. Background	
2.1 Exterior Wall Assemblies	Ritchey
2.2 International Building Code	Ritchey
2.3 Fiber Reinforced Polymers	Ritchey
2.4 NFPA 285	Cornachini
3. Literature Review	
3.1 FRP Thermal Properties and Fire Performance	Foley
3.2 An Experimental Study of Some Line Fires	Foley
3.3 Design of an Intermediate Scale Fire Test Rig	Foley
4. Project Approach	
4.1 Heat Transfer Partitioning	
4.1.1 NFPA 285 Calibration	Knight
4.1.2 Kreysler & Associates Evaluation Tests	Foley
4.2 Development of Source Fire	
4.2.1 Burner Design	Cornachini
4.2.2 Test Variations	Cornachini
4.2.3 Scaling Heat Release Rate	Knight
5. Results	
5.1 Temperature	Knight
5.2 Heat Flux	Knight
6. Analysis	Knight
7. Conclusions and Recommendations	Knight
Appendix A – IBC	Ritchey
Appendix B – Instrumentation	Foley/Knight
Appendix C – Exterior Wall Assemblies	Ritchey
Appendix D – Heat Transfer Partitioning	Foley/Knight
Appendix E – Fire Model of NFPA 285	Knight
Appendix F – Emissivity of Combustion Products Calculation	Knight
Appendix G – Test Data Burn 1	N/A
Appendix H – Test Data Burn 2	N/A
Appendix I – Test Data Burn 3	N/A
Appendix J – Test Data Burn 4	N/A
Appendix K – Test Data Burn 5	N/A
Appendix L – Gas Burner Background	Foley
Appendix M – FDS Input File	Knight

Abstract

Combustible materials offer great benefit to builders and architects be it aesthetics, thermal performance, cost, or ease of use. The use of combustible materials in exterior wall assemblies is regulated in the USA via the building codes to limit the potential for fire spread. Assembly acceptable performance is demonstrated based on evaluation in a standard test NFPA 285, the multi-story building test. NFPA 285 is a rigorous full scale fire test whose cost per test is high. This high cost severely limits its use by manufacturers for design iterations to optimize their products. Using a previously designed intermediate scale fire test rig, the goal of this project was to design a source fire for the rig that simulates the source fire characteristics of NFPA 285. By utilizing existing 2D plume theory, adapting heat transfer principles, and running fire models this project developed a rig source fire to replicate the thermal insult of NFPA 285 which will allow for economical testing related to assembly optimization.

Acknowledgements

The group would like to thank Professor Dembsey for his continuous direction and guidance throughout this project. The group would also like to acknowledge Kreysler & Associates for providing the test specimens and data from past testing which made our project possible. Finally, the group would like to thank the WPI Fire Protection Laboratory Manager, Randy Harris, for teaching the group proper safety procedures and instructing the team throughout the completion of the testing.

Content

List of Tables

List of Figures

1. Introduction

As the market for combustible material use in exterior wall assemblies develops, there is an increasing concern for the hazardous flame spread propagation characteristics of these materials. These characteristics are tested in accordance to standards set forth by the National Fire Protection Association (NFPA). The standardized test, NFPA 285, costs roughly $50,000 to complete and is conducted in a pass or fail manner. Since a specimen could fail the test within minutes, manufacturers are skeptical to test all of their products for fear of an expensive failure. A technique to accurately predict the material's ability to pass NFPA 285 is needed to give manufacturers confidence to innovate new products and dramatically progress the market. Throughout the course of this project, significant progress has been made towards making this technique a reality. By simulating NFPA 285 on an intermediate scale rig, the group has created the opportunity for manufacturers to test their material for under $10,000. Although this new testing method for exterior wall assemblies cannot replace NFPA 285, it does serve as an effective screening tool and offers an accurate prediction of whether or not a product would be able to pass the full scale test.[1]

Before the group began replicating the heat fluxes of NFPA 285, the plume that is affecting the specimen needed to be characterized. By drawing upon the works of previous Major Qualifying Projects (MQP), a determination was made that NFPA 285 could be characterized as nominally two-dimensional (2D).[2] Because of this assumption, the group was able to apply a set of equations, developed by Yuan and Cox, known as 2D Plume Theory.[3] The 2D plume theory was then utilized to collapse the data from various experiments and tests in the WPI Fire Protection Lab. The data correlation from the practice burns was then compared to the collapsed data from NFPA 285 to determine its degree of success. New data allowed the group to be able to adapt this theory to the experimental setup of this project. Finally, it was determined that this new refined theory could be applied to the intermediate scale rig.

Testing in the lab was completed on a nonflammable ten foot by four foot practice wall which was exposed to a plume created by a 28-inch line burner designed and fabricated by the group. The results of these burns were recorded by data acquisition software and analyzed to identify trends. Through heat transfer partitioning, design modifications and experimentation during this project, the first steps towards creating an effective screening test for NFPA 285 were taken.

2. Background

2.1 Exterior Wall Assemblies

Exterior wall assemblies are the outermost parts of any building. These walls must protect the rest of the structure, and its contents, from many different hazards. According to Lemieux and Totten, the three basic types of exterior walls are mass walls, barrier walls and cavity walls.[4] Mass walls are named so because they utilize the bulk mass of the wall to resist the passage of the elements. A barrier wall is very straightforward in that it provides a barrier between the outside elements and the inside of the wall through a water-tight system. The final type of exterior wall type, a cavity wall, utilizes an air gap in its construction in order to both resist water penetration as well as provide thermal insulation. In Appendix C more information is given about what goes into exterior wall assemblies and specific information about popular types of exterior wall assemblies.

Underwriter's Laboratories (UL), one of the primary listing agencies of the United States, has over 2000 unique wall assemblies listed for approved use in structures. These walls are all listed for a specific fire resistance rating as per ANSI/UL 263. Additionally for use in exterior walls, the assemblies are put through testing to determine their performance in terms of fire propagation (NFPA 285), water penetration (ANSI E331), and air leakage (ASTEM E2357).[5]

2.2 International Building Code

The International Building Code (IBC) regulates safe building practices throughout the world. Due to the copious amounts of information contained in the IBC, only some sections are suitable for this project. The IBC defines an exterior wall (also referred to as an exterior wall assembly) as "*A wall, bearing or nonbearing, that is used as an enclosing wall for a building, other than a fire wall, and that has a slope of 60 degrees (1.05 rad) or greater with the horizontal plane.*"[6] The code further defines some specific types of materials for use on exterior walls. These materials include wood, masonry, metal, concrete, glass-unit masonry, plastics, vinyl siding, fiber-cement siding, exterior insulation and finish systems (EIFS), and polypropylene siding. Additionally the IBC specifies that non-specified materials are permitted to be used provided that they are approved by the authority having jurisdiction.[6]

To make sure that these materials are safe, the IBC defines five separate performance requirements for exterior wall assemblies. These requirements include testing the weather protection, structural integrity, flood resistance, fire resistance, and flame propagation abilities of the given materials. The assemblies all have a specific set of regulations that are required for each respective material. As a result of the confusing nature of the IBC and how each material is required to meet slightly different regulations, another method of utilizing the IBC, which lays out the regulations in a easier to follow format, is included in Appendix A.

2.3 Fiber Reinforced Polymers

Fiber Reinforced Polymers (FRP) is a recently emerging material that has started to become a popular choice for exterior wall assemblies. Typically, the composition of FRP is a polymer matrix or resin reinforced with fibers such as glass.[6] Other materials such as fillers and additives can be added but they are not essential. The material for the matrix can be any plastic; in general, it is a syrupy liquid which combined with a hardener forms a cross-linked solid. The composite is ready after adding fibrous material to the matrix in the form of a cloth and allowing the resin to cure. This process occurs in a closed or open mold. The addition of fibrous materials enhances the strength and elasticity of the resultant polymer. Nevertheless, the properties of the final material depend on the mechanical properties of the matrix and the fiber, their ratio, and the length and orientation of fibers in the matrix.[7] Due to the variance in the potential properties of FRP, they need to be tested extensively to confirm their safe usage.

2.4 NFPA 285

NFPA is one of the world's leading publishers of codes and standards to reduce the potential for fire-related risks. NFPA 285 was created in the late 1970's with the proposal of foam plastic (a combustible material) for use in exterior, non-load-bearing walls on noncombustible construction (typically Types I, II, III, and IV).[8] The definition of NFPA 285 is as follows:

> *"This standard provides a test method for determining the fire propagation characteristics of exterior non-load-bearing wall assemblies and panels used as components of curtain wall assemblies, that are constructed using combustible materials or that incorporate combustible components, and that are intended to be installed on buildings required to have exterior walls of noncombustible construction."*[8]

The purpose of NFPA 285 is to provide a standardized test procedure for evaluating the aforementioned walls, on buildings that are required to be non-combustible. These walls are tested for:

1. The ability of the wall assembly to resist flame propagation over the exterior face of the wall assembly
2. The ability of the wall assembly to resist vertical flame propagation within the combustible components from one story to the next
3. The ability of the wall assembly to resist vertical flame propagation over the interior surface of the wall assembly from one story to the next
4. The ability of the wall assembly to resist lateral flame propagation from the compartment of fire origin to adjacent compartments or spaces[8]

The test itself consists of a two story concrete structure, with the exterior assembly mounted onto its front face. The building has two vertically stacked rooms, in the center of the lower room there is a burner which is used to replicate a fire burning inside of the room. The lower room has a single window in the test specimen, where another burner is positioned to replicate the fire spilling out of the window.[8]

NFPA 285 has six 5-minute steps where the thermal insult to the assembly is increased. To determine the exact gas flow rates needed and the placement of the burner, there is a calibration procedure which helps eliminate any differences caused by the slightly different setups and conditions that different facilities may have. For example, the ambient temperature can vary up to 40 degrees Fahrenheit, and the relative humidity can vary between 20% to 80% in the test facility.[8]

The calibration specifies six temperature values and three heat flux values at one foot increments above the window. NFPA 285 also has a range of other instruments used in the evaluation of a test specimen. However, the nine aforementioned instruments are the only ones used in the calibration procedure. Temperature values are acceptable within ten percent, and heat fluxes are acceptable within an average of twenty percent.[8]

Acceptance criteria for NFPA 285 includes:

- No vertical and horizontal flame spread outside of the impingement zone on the exterior face
- No vertical and horizontal flame spread in the combustible components/insulation
- Maximum temperature in second story test room (500 degree Fahrenheit)
- No flames in second story test room
- No flame spread to sidewalls of apparatus[8]

3. Literature Review

3.1 FRP Thermal Properties and Fire Performance for Building Exterior Applications

The MQP completed by Jacob Czarnowski, Kristen Nich and Kristina Zichelli examines the increasing application of fiber reinforced polymers (FRP) in exterior wall assemblies. The uses of these products are expanding because of their versatility and simplicity of installation, however concerns have emerged regarding the material's flame spread characteristics. Using data collected from Cone Calorimeter testing in accordance to ASTM E1354, the group was able to estimate the thermal properties of fiber reinforced polymers in its early heating stages. By utilizing 2D spill plume theory and data collected from NFPA 285 tests of the FRP, the group was able to predict flame height through the use of Cone Calorimeter testing. The data collected in the cone was then applied to 2D plume theory and used to create a method for modeling the performance of FRPs. This method was then compared to the values obtained by the NFPA 285 tests of the same material provided by Kreysler and Associates. This validated

the claim that NFPA 285 could be considered nominally 2D. The group's work provides manufacturers the ability to predict the outcome of NFPA 285 tests while reducing the cost of material development.[2]

3.2 An Experimental Study of Some Line Fires

This study by Li-Ming Yuan and G. Cox examines the elements of line fires and represents complex situations in an idealized two-dimensional format. The research paper describes the laboratory-scale experiments conducted on line fires and reports measurements of gas temperature, gas velocity and visual flame heights.[3]

The line fires in these experiments were produced using three different burners. These burners consisted of two porous refractory burners, 0.2 meters and 0.5 meters long, as well as a 0.5 meter long sand box burner. The width of the burner slot ranged from 15 millimeters to 50 millimeters wide and each burner was elevated 0.7 meters above the floor. The natural gas supply was adjusted to provide a theoretical range of heat release rates between 2 kilowatts and 110 kilowatts. A fine mesh screen was fit around the rig to limit the effects of ambient air movements.[3]

Yuan and Cox used the data collected in their experiment to satisfy their claim of different flame regions within a plume:

> *"The rising plume of flame and buoyant gases above a fire has been shown in several studies of the analogous axisymmetric system to be divided vertically into three distinct regions associated with 'continuous' and 'intermittent' flaming regions closest to the source, and a 'convectional buoyant plume' above the flame tips."*[3]

Using appropriate scaling for turbulent line fires, the normalized centerline time-mean temperature and velocity measurements recorded are shown in Figure 1 and Figure 2.

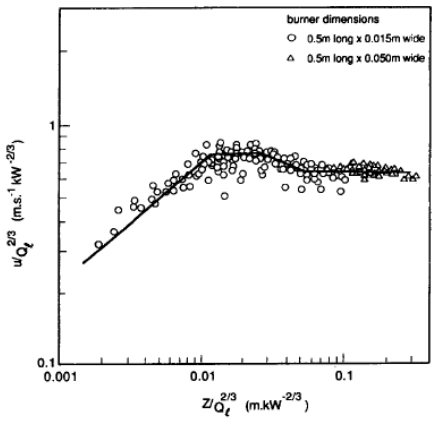

Figure 1 - Reduced Centerline Velocity with Height[3]

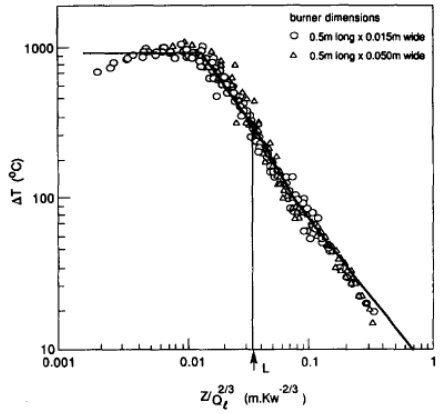

Figure 2 - Centerline Temperature Rise with Reduced Height[3]

Theoretical heat release rate (Q'), height above burner (z), and flame height (L) have significant impacts on the characteristics of the 2D plume region. The continuous region of this asymmetrical case is described as $z/(Q^{2/3}) \leq 0.015$ or $z/L \leq 0.5$. The intermittent flame is described as $z/(Q^{2/3}) = 0.034$ while z/L ranges from 0.5 to 1. The final convectional plume flame region is described as $z/(Q^{2/3}) = 0.2$ while z/L ranges from 1 to 6.[3]

Each of these three flame regions have specific dimensionless constants, B and n, which are used to calculate the centerline temperature using the equation below.[3]

$$\Delta T_m = B(z/Q_1^{2/3})^{2n-1} \quad \textbf{(1)}$$

3.3 Design of an Intermediate Scale Fire Test Rig for Exterior Wall Assemblies

The MQP completed by Christoper Ciampa, Ethan Forbes and Ditton Kawalya identified shortcomings of the standard NFPA 285 test. To resolve the high expense and time consuming nature of the full scale test, this project proposed the development of an intermediate scale fire test rig for screening fire behavior of exterior wall assemblies. The rig designed by the group would dramatically reduce the size and cost of test specimens which would benefit manufacturers by providing them insight into the performance of their assembly.[1]

The group identified the current flaws of NFPA 285 to be price, size, portability, construction, and test time. The project also compared NFPA 285 with their potential solution:

> *"If the problems from the current testing rig can be solved then a much more efficient setup can be designed. A more portable, affordable and faster testing rig would benefit many people in the industry. Reducing the size and cost of the test will allow researchers to pre-screen the performance of their materials before a full-scale test hence avoiding unnecessary money and time expenditure."*[1]

This MQP designed a steel rig which could simulate the most common failure point of an NFPA 285 test on a ten foot by four foot wall specimen. Since the test rig would not have a window opening, it was designed to have side channels which could be used to help match the vertical gas flow exhausting from NFPA 285's window opening. Steel was chosen because of its ability to withstand the heating of the burner as well as support 1,000 pounds wall sections. Since ease of assembly was critical to the project, locking pins are used to assemble the wall without the use of tools. The assembly procedure is shown in Figure 3 below:

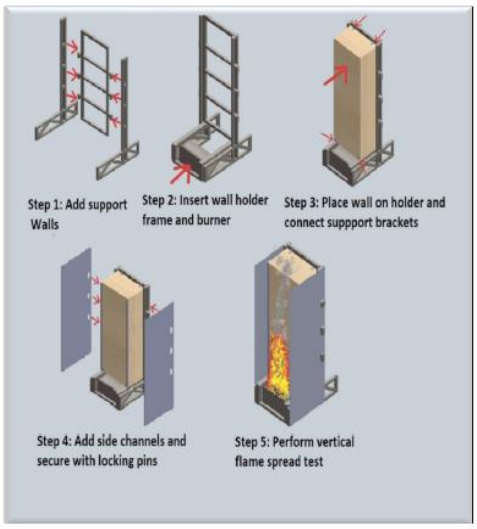

Figure 3 - Rig Assembly Steps[1]

The design of this rig was then fabricated by the project's sponsor, Kreysler and Associates, and became the fundamental design guideline in the development of the group's burner.

4. Project Approach

4.1 Heat Transfer Partitioning

4.1.1 NFPA 285 Calibration

In order to accurately compare the fire of NFPA 285 and that of the designed burner, it was necessary to characterize NFPA 285 in terms of the plume which the test specimen is exposed to. This characterization comes primarily from the calibration provided within NFPA 285 as well as existing work completed by Czarnowski et al.[2]

NFPA 285 provides external plume centerline temperature data for one to six feet above the top of the window frame, and heat flux data for two to four feet above the window frame. Utilizing the existing 2D and spill plume theory, Czarnowski et al. determined that the flow resulting from the dual burner arrangement of NFPA 285 could be considered nominally a 2D Spill Plume. Next it was necessary to characterize the plume of an NFPA 285 calibration in terms of the modes of heat transfer between the resultant plume and the wall specimen. To do this fundamental radiation and convection heat transfer equations were utilized, along with data from the calibration procedure. Utilizing the calibration heat flux values from NFPA 285, the total heat flux to the three locations along the centerline of the wall was known. The equation for total heat flux is

$$q''_{total} = q''_{conv} + q''_{rad} \quad \textbf{(2)}$$

Using the equations from the Society of Fire Protection Engineers (SFPE), the emissivity of the methane fire plume of NFPA 285 was determined to be 0.112. Appendix F provides details on this calculation. With this emissivity known, the radiation heat transfer equation was used

$$q''_{rad} = \varepsilon \sigma T^4 \quad \textbf{(3)}$$

Where q" is the radiative heat flux in kW/m^2, epsilon is the emissivity of the fire plume, sigma is the Stefan-Boltzmann constant, and T is the temperature of the plume from calibration data. Next the radiative heat flux was subtracted from the net heat flux values to determine the convective heat flux. Finally, the convective heat transfer equation was used to determine the convective heat transfer coefficient of the plume.

$$h_c = \frac{(T_{plume} - T_\infty)}{q''_{conv}} \quad \textbf{(4)}$$

Table 1 is a sample the heat flux calculations used for the 10-15 minute time step.

Table 1 - Sample Heat Flux Calculation Values

NFPA 285 Calibration 10 - 15 Minutes					
Nom. Height [ft]	**Tplume [C]**	**q" [kW/m^2]**	**q"rad [kW/m^2]**	**q"conv [kW/m^2]**	**hc [W/m^2K]**
2	605	25.00	3.79	21.21	36.26
3	591	26.00	3.55	22.45	39.31
4	528	20.00	2.63	17.37	34.20

Figure 4 shows the heat transfer experienced at two feet above the window in terms of its components. Throughout all three available heat flux measurements the average ratio of convection to radiation was 87:13. Full results from the calculations can be found in Appendix D.

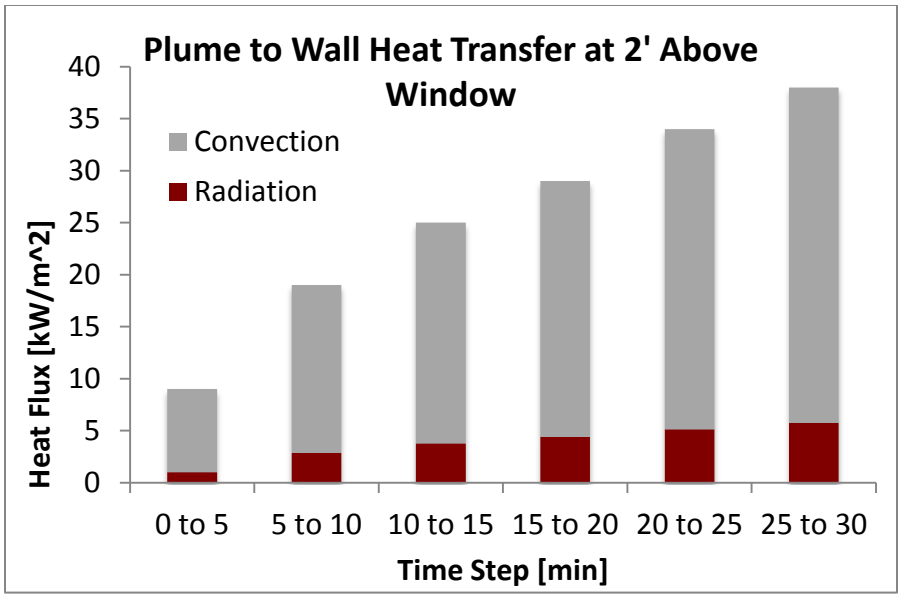

Figure 4 - NFPA 285 Heat Transfer Partition

4.1.2 Kreysler & Associates Evaluation Tests

After characterizing the plume heat transfer using the values obtained from the NFPA 285 calibration procedure, the same equations were used to characterize the heat transfer of the evaluation tests in the NFPA 285 reports provided to the group by Kreysler & Associates. Unlike the calibration in NFPA 285, heat fluxes were not recorded. Therefore, the group used the convective heat transfer coefficients of the NFPA 285 calibration calculations. Using Equations 3 and 4, the group determined the radiative and convective heat fluxes respectively. The emissivity used in Equation 3 was that of propane in an attempt to account for the greater sooting of the test specimen. Appendix F has details of this calculation.

The recorded heat flux values at two feet above the window burner for this evaluation test are shown in Figure 5.

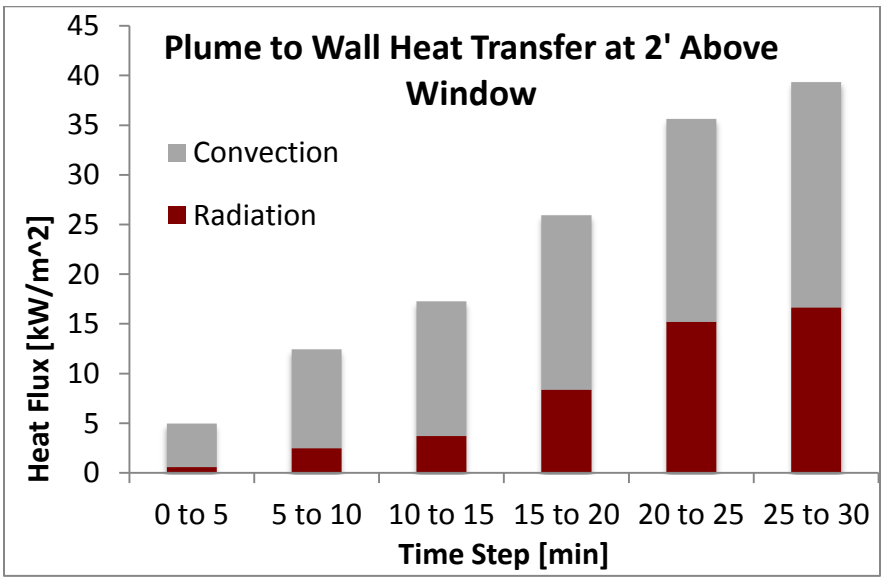

Figure 5 - Kreysler Evaluation Test Heat Transfer Partition

The total heat flux values obtained from the evaluation test followed a similar trend to the NFPA 285 calibration heat flux data. The primary difference is the larger radiative heat flux values in the evaluation test. This was expected because the evaluation test has the additional heat source of the burning wall which provides more radiation.

4.2 Development of Source Fire

4.2.1 Burner Design

Since the NFPA 285 test can be characterized as a 2D plume, this means that the smoke plume created is only considered to exist in two directions, height and width, and it is assumed to be infinitely long in the third direction. For this reason, a line burner was chosen as the type of burner for this project. A line burner is a cylindrical pipe with a straight slot cut out along its length. A mesh screen lines the slot to diffuse the gas as it exits the burner, where it is ignited to create a non-premixed flame.

The burner was designed for this project to resemble the window burner from NFPA 285 as closely as possible. For this reason, the pipe diameter and slot thickness were maintained from NFPA 285, while the slot length needed to be scaled down from 48 inches to fit in the intermediate rig assembly. This resulted in a final slot size of 0.5 inches by 28 inches. The main two inch pipe is fed on both sides by symmetric one inch diameter steel piping to ensure even gas flow. The burner assembly is shown in Figure 6.

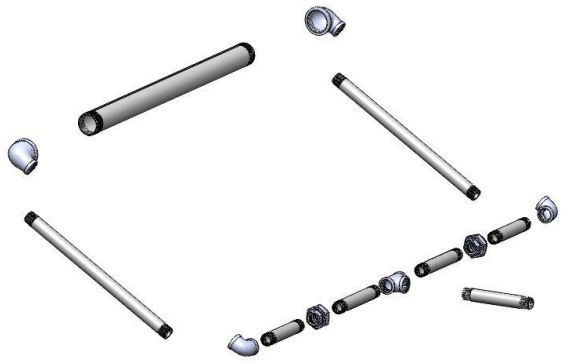

Figure 6 - Burner Assembly

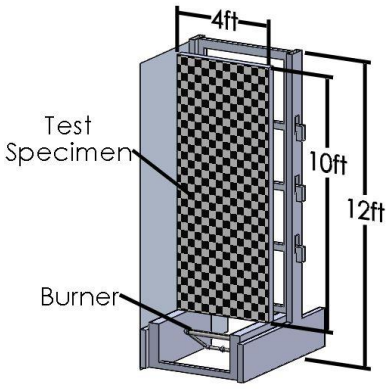

Figure 7 - Test Rig Assembly

4.2.2 Burn Variations

A temporary practice wall and rig were constructed to allow the group to perform burns before the intermediate scale rig assembly was ready for use. The temporary rig raised the wall 15 inches, and featured a fireproof compartment below the wall that was 36 inches wide, 16 inches deep, and extended down to the floor. This compartment was sealed for all burns except number two. Sealing the compartment removed any thermal insult on the bottom of the wall (the theoretical “top” of the window sill), and isolated the exterior face of the wall. This allowed the group to focus on replicating the temperature and heat flux values provided in the NFPA 285 calibration procedure.

Throughout testing, the burner’s orientation was changed in order to determine its optimal placement to provide the most consistent thermal insult on the wall. The horizontal distance from the burner to the exterior face of the wall was varied throughout testing. Table 2 shows the variations of each burn. The optimal dimensions were determined to be 9 inches below, 1¾ inches horizontally, and centered along the length of the slot.

Table 2 - Burn Variations

Burn #	Horizontal Offset (Inches in front of wall)	Vertical offset (Inches below wall)	Use of Compartment	Burn Duration (min)	Heat Release Rate (kW/m)	Fuel Flow Rate (SCFM)
1	+5	9	No	20	467-1143	9.0-22.0
2	+5	9	Yes	38	52-545	1.0-10.5
3	+3	9	No	12	126-308	2.4-5.9
4	+2	9	No	12	248-896	4.8-17.3
5	+2	9	No	12	290-657	5.6-13.0

Although NFPA 285 uses natural gas, propane gas was used for testing because it has a higher soot yield and is more readily available in the WPI Fire Protection Laboratory. A higher soot production is beneficial to this project because it increases the radiative heat flux produced by the burner. This is necessary because the combined plume created by the room and window burners in NFPA 285 carries more convective heat flux than can be produced by the single burner designed for this project. For this reason, radiative heat flux produced by soot can be used to supplement some of the missing heat flux. Table 3 compares some of the chemical properties of methane and propane.

Table 3 - Methane vs Propane[9]

Property	Methane	Propane
Chemical Formula	CH4	C3H8
Density (kg/m^3)	.668	1.882
Heat of Combustion (kJ/g)	50.00	46.45
Soot Yield (g/g)	0.000	0.024
Flame Temp (K)	1446	1554
Soot Volume Fraction	4.49E-6	7.09E-6
Total Calculated Emissivity	0.112	0.188

4.2.3 Scaling Heat Release Rate

Over the course of the project a variety of heat release rates were tested to gather enough data in order to properly characterize the line burner. The heat release rate values provided in NFPA 285 were scaled to produce an equivalent heat release rate per unit length in the intermediate scale rig. The length scale used for NFPA 285 was the length of the window (1.98 meters) and the scale used for the intermediate scale rig burner was the slot length (0.71 meters). Since the intermediate scale rig burner uses propane as a fuel, the associated heat of combustion and density were used to convert to the required flow rates after the heat release rates were scaled.

The heat release rate values for the window, room and combined burners of NFPA 285 were all scaled to the intermediate scale rig burner and those values are summarized below. Due to the differing

geometries and flow conditions of the intermediate scale rig and the single burner set up, these scaled heat release rates did not produce temperature or heat flux values exactly equivalent to an NFPA 285 calibration.

Table 4 - Scaling Flow Rate from NFPA 285 to Rig Burner

Window Burner Flow Rate (CFM)		
Time Step	**NFPA 285**	**Equivalent in Rig**
0 to 5	0	0.00
5 to 10	9	1.59
10 to 15	12	2.11
15 to 20	16	2.81
20 to 25	19	3.34
25 to 30	22	3.87
Room Burner Flow Rate (CFM)		
Time Step	**NFPA 285**	**Equivalent in Rig**
0 to 5	38	6.68
5 to 10	38	6.68
10 to 15	43	7.56
15 to 20	46	8.08
20 to 25	46	8.08
25 to 30	50	8.79
Combined Flow Rate (CFM)		
Time Step	**NFPA 285**	**Equivalent in Rig**
0 to 5	38	6.68
5 to 10	47	8.27
10 to 15	55	9.67
15 to 20	62	10.89
20 to 25	65	11.42
25 to 30	72	12.66

5. Results

5.1 Temperature

The temperature profiles of all the burns, shown in Figure 8, are scaled by the height above the burner divided by the heat release rate per unit width to the $^{2}/_{3}$ power, following the precedent set by Yuan & Cox. The black line displays the theoretical temperature rise as correlated by Yuan & Cox. As can be seen the data from the burns collapse well about the correlation with some notable variation. Burn 1 has higher values, which is considered to be due to the presence of the paper on the gypsum board burning

for a majority of the experiment. The fit of the data is stronger when you consider that contained within this graph are three separate burner spacings and two wall geometries.

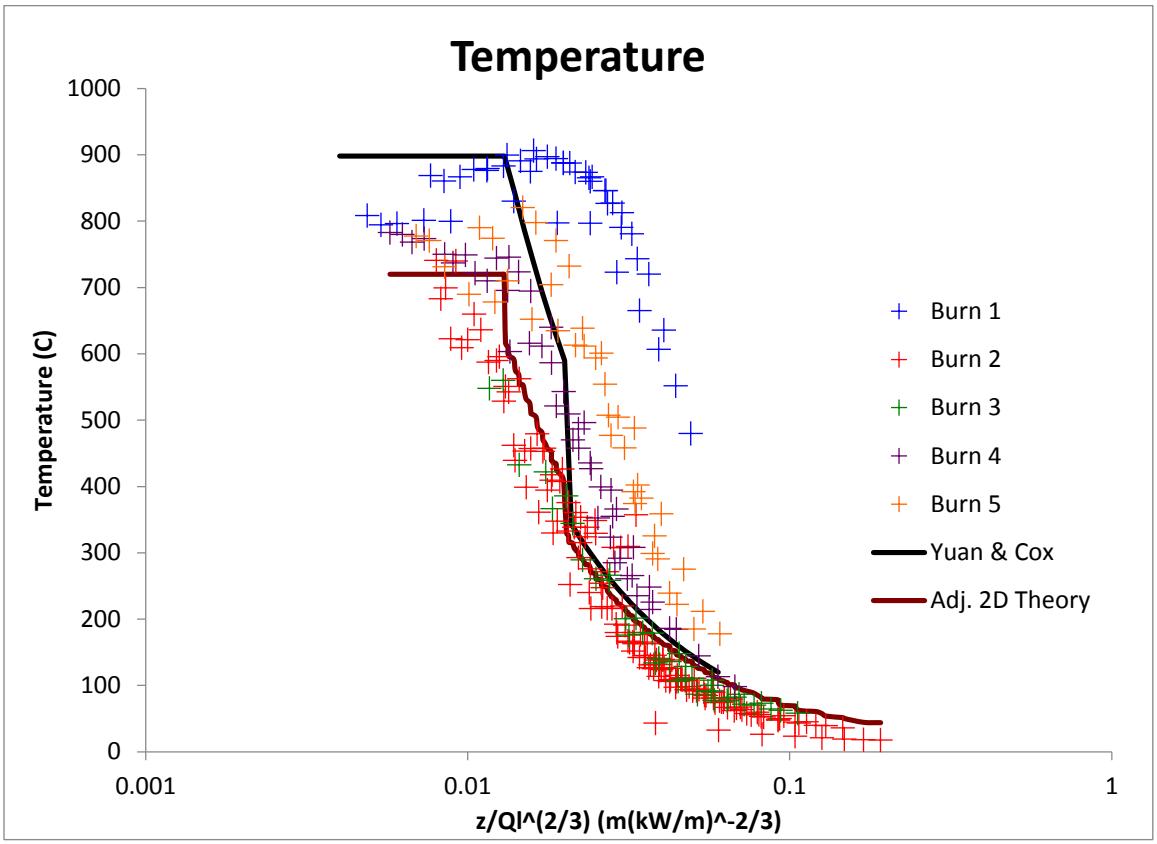

Figure 8 - Temperature Profile (All Burns)

By leveraging the existing 2D plume theory, the team was able to fit a correlation to the results by imposing the physical constraints of the three flame regions, continuous, intermittent and plume upon the data. The correlation was fit using an average error minimization technique. Burn 1 was not included in the data because of the inflated values due to drywall paper combustion. The form of Yuan & Cox's equation was replicated, keeping the exponential constants the same and varying the coefficient B. Table 5 provides the adjusted constant values for the temperature correlation. This correlation adjusts the existing theory based upon a burner in the open to a line burner against a vertical face.

Table 5 - Temperature Correlation Constants

Plume Region	Yuan & Cox B	Adjusted B
Continuous	898	750
Intermittent	11.8	8
Plume	7.2	6.5

5.2 Heat Flux

The heat flux profiles of all burns are shown in Figure 9, again plotted on the X-axis by Yuan & Cox's scaling variable. The heat flux profile follows a trend, however no existing correlations exist for comparison. Notably, as opposed to Yuan & Cox's temperature correlation, heat flux does not appear to have as obvious a maximum value in the continuous flame zone. Again this data represents the same experimental variation as the temperature profile, so there is strong consideration to the collapsing of the data about one profile.

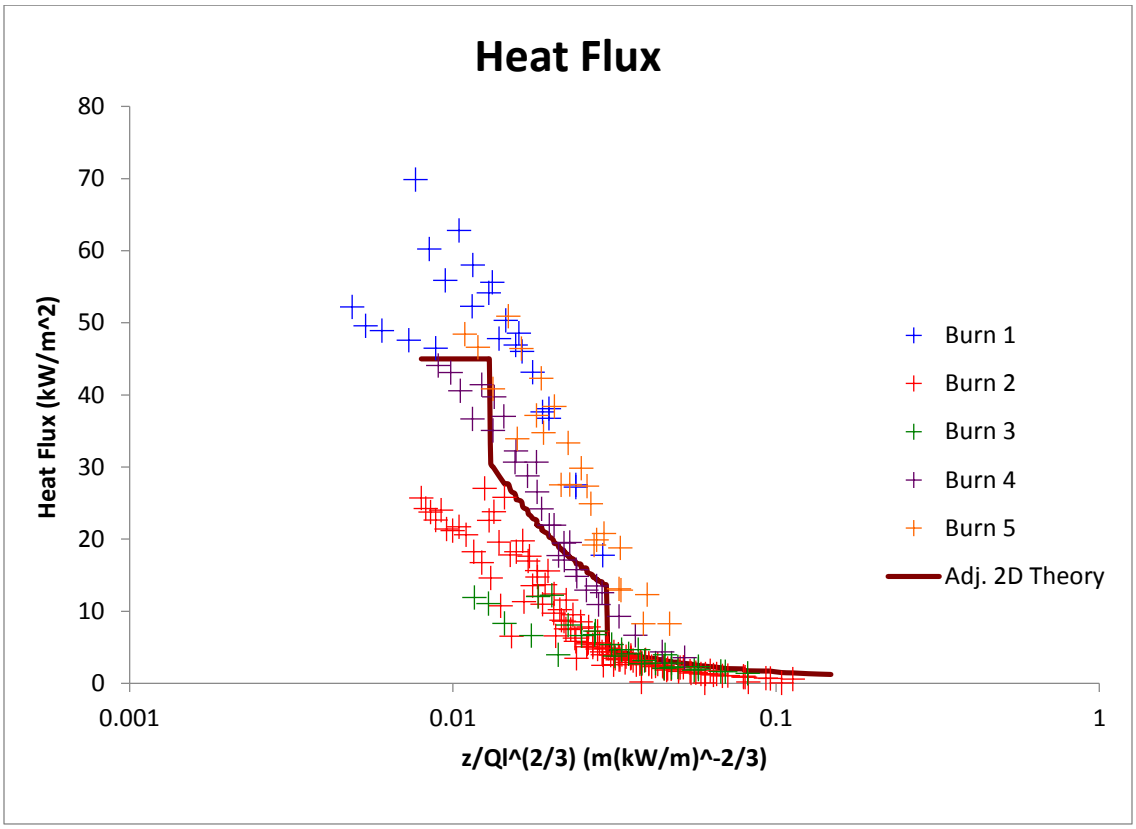

Figure 9 - Heat Flux Profile (All Burns)

The same method was used to create a correlation for heat flux as was done with temperature. Heat flux was not correlated in Yuan & Cox's work, however because of its direct relation to temperature the same form of the equation and physical constraints were used. Table 6 provides the adjusted constant values for the heat flux correlation. Again the exponential constant, n, remains the same as Yuan & Cox.

Table 6 - Heat Flux Correlation Constants

Plume Region	Adjusted B
Continuous	45
Intermittent	0.4
Plume	0.14

6. Analysis

When viewed in aggregate, the data from the entirety of the experimentation performed by the group provides strong support that the burner produces a flame and plume which can be considered 2D. As can be seen in the results the data collapses well around the existing theory, which is based upon experiments of a line burner in the open. By adjusting the theory slightly, the group is able to provide a correlation for a line burner against a vertical face.

Using the compilation of the data from the five burns completed, the group has isolated six unique time steps which provide the best match to NFPA 285 values. These values were chosen by determining which fuel mass flow rate produced the closest heat flux at the three foot calorimeter of the NFPA 285 calibration. Since the temperatures of NFPA 285 are measuring a gas temperature, the heat flux was chosen as the goal because it more accurately determines how the wall experiences the thermal effects of the flame and plume.

The choice of the three foot heat flux value requires some explanation of a key difference between the plume of the intermediate scale rig and NFPA 285. Due to the mass of hot gases exiting the burn compartment of NFPA 285, the measurements closer to the window frame are reported as lower than those farther up. Fire plume theory states that the centerline temperature measurements should be at a maximum closest to the origin of the fire and decrease in magnitude as you ascend vertically up the plume. The reason for the divergence of NFPA 285 from the theory is what the group has defined as “Exit Effects”. This is due to the momentum of the compartment exhaust separating the thermal boundary layer away from the wall horizontally, before it eventually attaches to the wall further up the face. This can be evidenced by every one foot and some two foot temperature measurements being less than those immediately above it, and every two foot heat flux measurement being less than the three foot measurement in an NFPA 285 calibration. Due to this, the group did not deem it possible to replicate these values with a line burner against a vertical face; the group has conceded that the first temperature and heat flux measurement are unlikely to be matched. The “Exit Effects” are highlighted in Figure 10 and Figure 11 as the blue data points.

When considered as an absolute average, the burner was able to reproduce temperatures and heat fluxes to within 19% and 23% of NFPA 285 respectively. When you discount the points deemed “Exit Effects” this accuracy improves to 14% and 13%. Finally, in the initial time step of NFPA 285 only the room burner is ignited. This profile is highly difficult to replicate with a single line burner, and when removed from the data set the accuracy of the results improves further to 11% for each. Table 7 provides the associated six flow rates and Figure 10 and Figure 11 compare NFPA 285 and the plume produced by those six flow rates in the burner.

Table 7 - Recommended Burner Regime

NFPA 285 (min)	Burner (CFM)
0 to 5	4.7
5 to 10	6
10 to 15	7.5
15 to 20	12
20 to 25	13.6
25 to 30	15

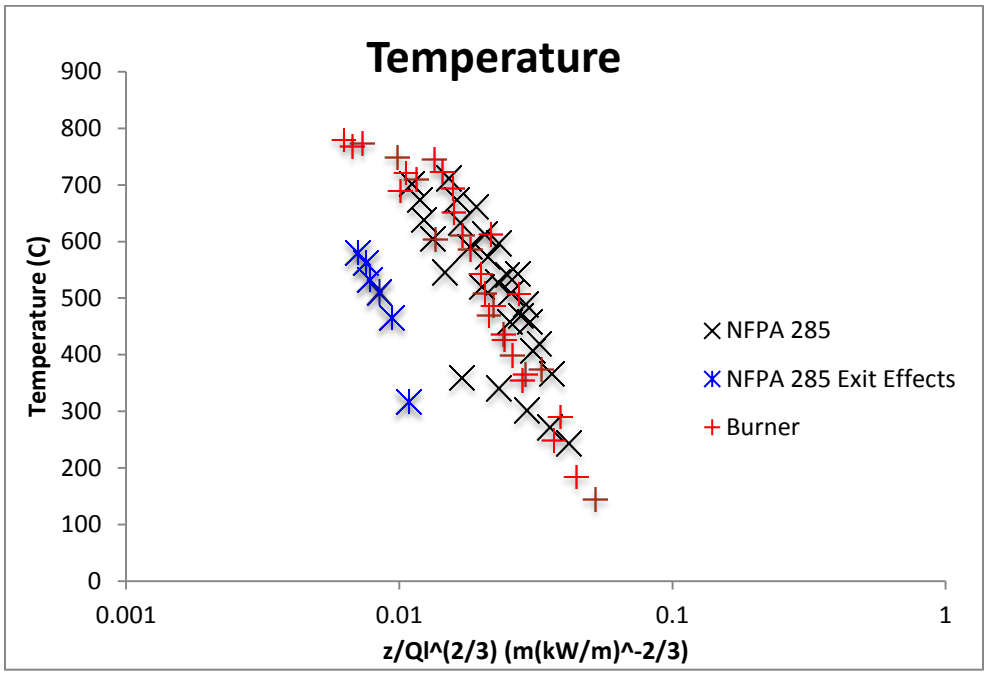

Figure 10 - Recommended Burner Regime vs NFPA 285 - Temperature Profile

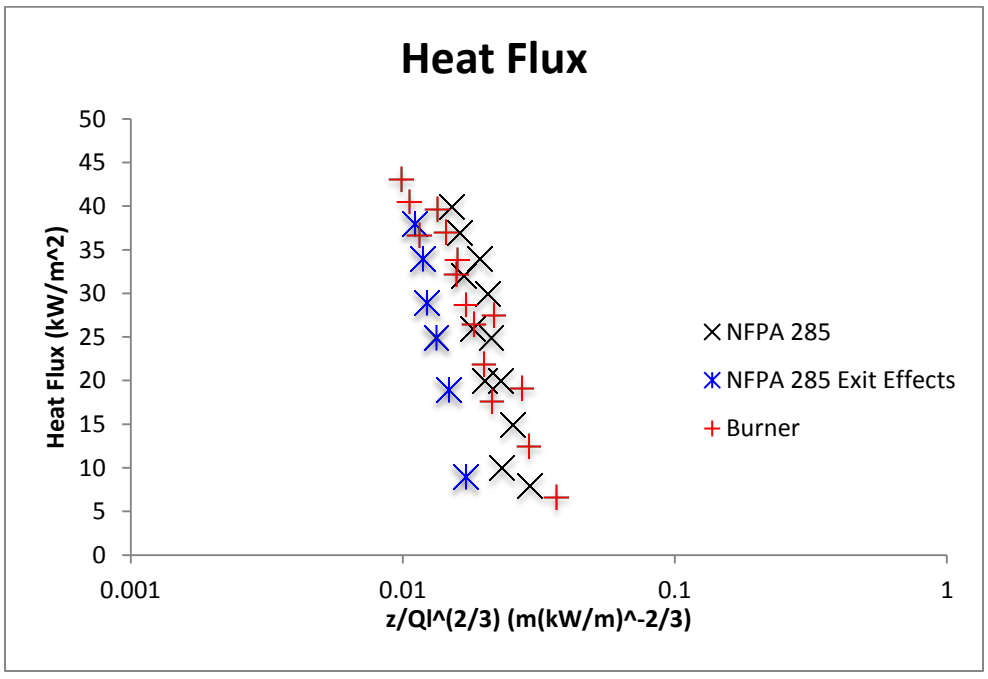

Figure 11 - Recommended Burner Regime vs NFPA 285 - Heat Flux Profile

The profiles produced by the burner differ slightly from those of NFPA 285 in shape. The compartment exhaust of NFPA 285 also contributes to the shape of the profile, making them slightly more uniform as height above the window increases. The burner's resultant profile had a steeper slope than that of NFPA 285, being more severe initially, but decaying more rapidly in magnitude as height increases. Figure 12 provides an example profile at the 10 to 15 minute time step to better visualize this effect.

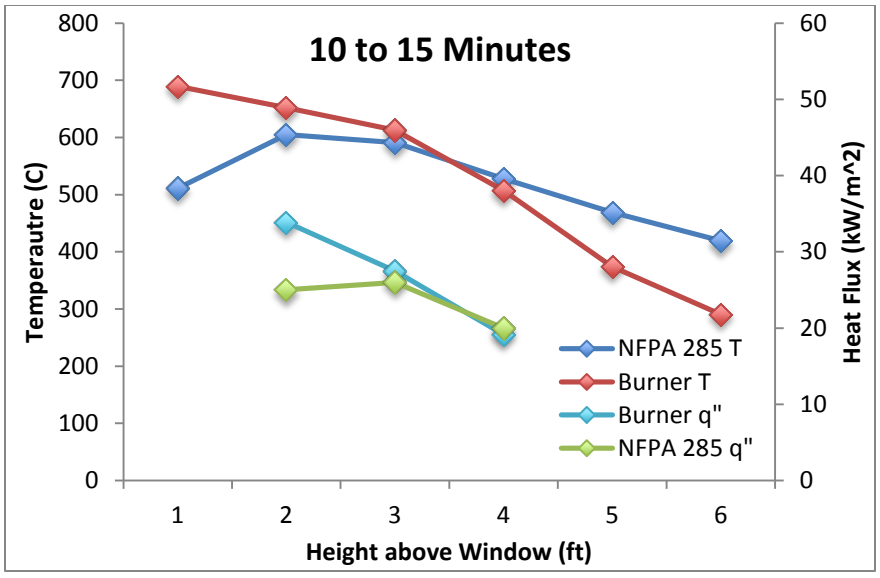

Figure 12 - Recommend Burner Regime vs NFPA 285 - Temperature and Heat Flux Profile - 10 to 15 min

The group originally investigated computer modeling NFPA 285 with Fire Dynamics Simulator (FDS) in order to more accurately determine the heat flux experienced by the top of the window frame, as this portion of the test specimen was identified as a typical failure point. However, in the process of running these models the group identified that the FDS runs, when combined with the experimental results, provide supporting evidence that the plume of NFPA 285 is highly dependent upon the presence of the window burner. Figure 13 and Figure 14 display sample profiles from an FDS simulation of NFPA 285 as tested and simulations isolating both the window and room burners. As can be seen, the magnitudes of both temperature and heat flux are highly dependent upon the presence of the window burner. Appendix E contains a more complete discussion of the FDS modeling completed by the group.

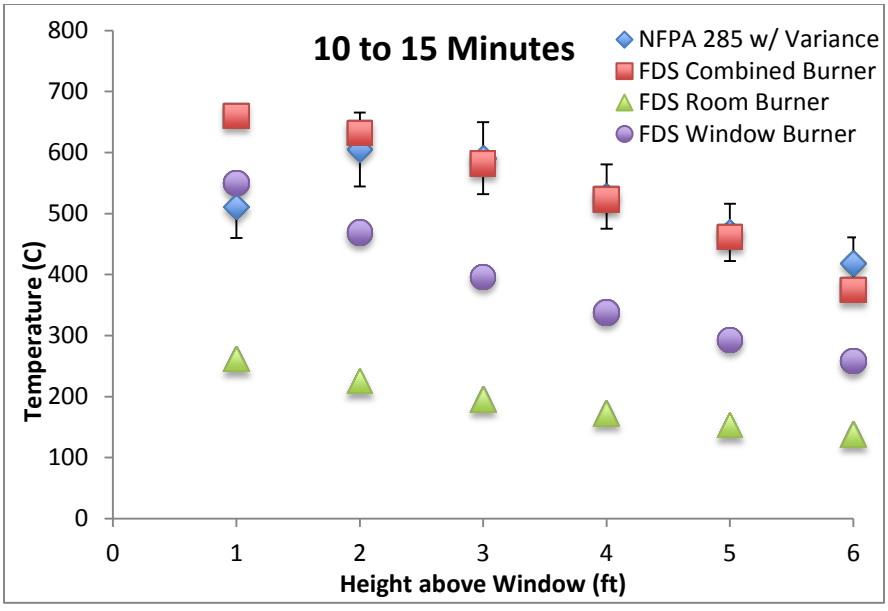

Figure 13 - FDS Simulation vs NFPA 285 - Temperature

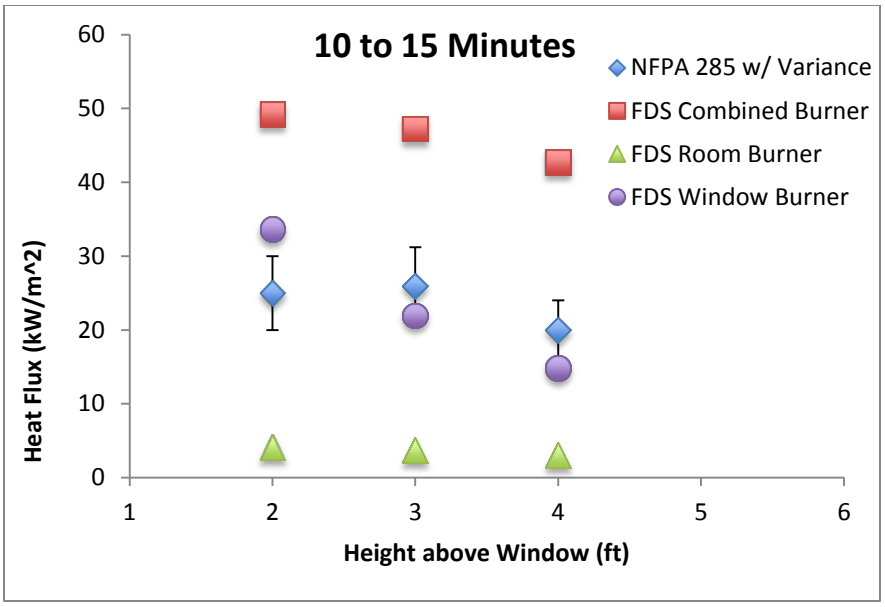

Figure 14 - FDS Simulation vs NFPA 285 - Heat Flux

Due to the large amount of moving gas, NFPA 285 has a large portion of convective heat transfer, with an average of 87% of thermal insult being due to convection. The group recognized that this level of convection was unlikely in the line burner and utilized the higher sooting properties of propane to make up for the lower level of convection with increased radiation. This corresponded to approximately 77% of heat transfer being appropriated to convection with our burner. Figure 15 displays the heat transfer partitioning at three feet between NFPA 285 and the groups recommended burner regime.

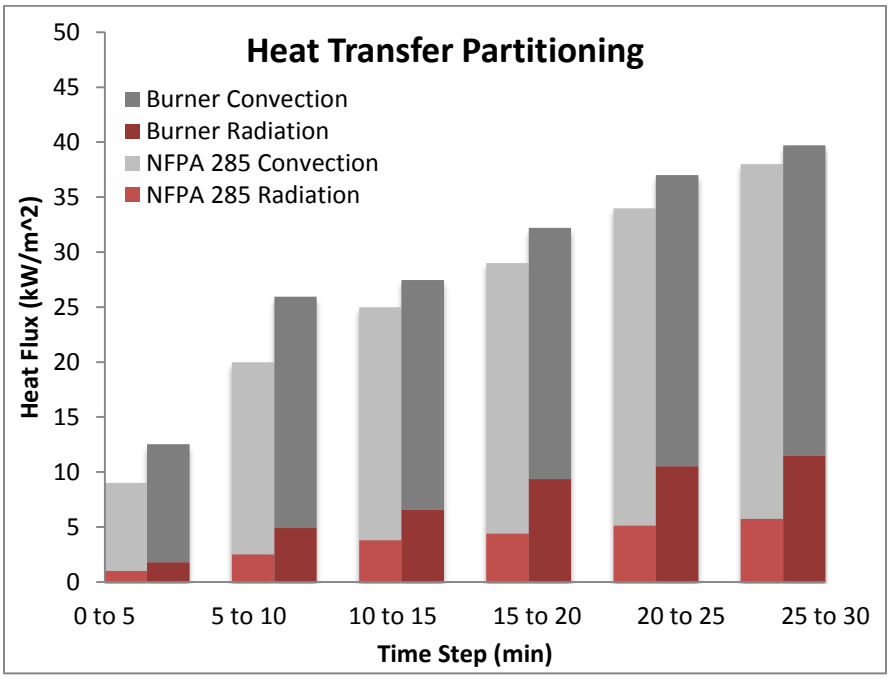

Figure 15 - Recommended Regime vs NFPA 285 - Heat Transfer Partitioning 3 Feet

7. Conclusions and Recommendations

In summary, the group is confident that the burner, when combined with the recommended flow rate regime, is capable of providing an accurate screening tool for exterior wall assemblies. Both NFPA 285 and the burner can be considered nominally 2D and the data is reproduced closely to NFPA 285 with the exception of the "Exit Effects". While temperature values differ above 10%, the acceptable range of a NFPA 285 calibration, the difference is intentional because when combined with a greater sooting fuel, it allows for radiation to make up for the lack of convection produced with the single burner. Heat flux values are reproduced to within 11%, which is just outside of the 10% measurement uncertainty of the instruments, and within the average 20% acceptance range of NFPA 285.

The group has three recommendations for future research in the development of the intermediate scale rig.

1. Testing of Other Burner Orientations

The group recommends investigating the use of this burner to more accurately reproduce the profiles of NFPA 285 by utilizing a different burner orientation. The burner is highly adaptable, being capable of adjustment in both height and slot orientation. The group recommends placing the burner in a noncombustible compartment located under the test specimen and attempting to create an outflow from said compartment. This quasi-exhaust flow should help in providing some convective heat transfer to create a more uniform temperature and heat flux profile.

2. Encourage More Data Gathering of NFPA 285

While the calibration procedure of NFPA 285 provides sufficient data to ensure that a test facility can replicate the scenario intended, there is a lack of data when it comes to accurately characterizing the resultant plume of NFPA 285. The heat flux profile matched by the group only contains three points, which does not provide a high rate of confidence for matching. Additionally, it creates a blind spot further up the test specimen as it is unclear as to what heat fluxes are being experienced beyond four feet above the test specimen. Finally, a common area of failure in NFPA 285 tests is the top of the window frame. This area is under thermal attack from the exhaust flows. However, no data is available to determine exactly what this thermal insult is.

3. Investigate the Effect of the Room Burner

The fire modeling completed by the group shows strong evidence that the magnitudes of the temperature and heat flux profiles resultant from NFPA 285 are highly dependent upon the presence of the window burner. The group recommends that additional research be completed into the exact effect of the room burner, in order to both more accurately replicate the temperature and heat flux profiles with a single burner as well as further investigate the thermal attack at the top of the window frame.

References

[1] Ciampa, Christopher, Ethan Forbes, and Ditton Kawalya. "Design of an Intermediate Scale Fire Test Rig for Exterior Wall Assemblies" (April 2014), Worcester Polytechnic Institute.
[2] Czarnowski, Jacob, Kristen Nich, and Kristina Zichelli. "FRP Thermal Properties and Fire Performance for Building Exterior Applications" (April 2013), Worcester Polytechnic Institute.
[3] Yuan, Li-Ming, and G. Cox. "An Experimental Study of Some Line Fires." Fire Safety Journal 27.2 (1996)
[4] Lemieux and Totten. "Building Envelope Design Guide - Wall Systems" National Institute of Building Sciences, (Aug. 2010), Accessed at http://www.wbdg.org/design/env_wall.php#funda
[5] Underwriters Laboratories. "Building Code - Exterior Walls" (Sept. 2014), Accessed at http://ul.com/code-authorities/building-code/exterior-walls/
[6] International Building Code. (2012 Edition). Washington DC: International Code Council.
[7] ASM Desk Editions: Engineered Materials Handbook 10th Edition.
[8] NFPA 285: Standard Fire Test Method for Evaluation of Fire Propagation Characteristics of Exterior Non-Load-Bearing Wall Assemblies Containing Combustible Components, (2012 Edition). National Fire Protection Association, Quincy MA.
[9] SFPE Handbook, 3rd Edition, Society of Fire Protection Engineers, Quincy MA, (2002)

Contents

Appendix A – IBC Flowchart

Acknowledgements

Special thanks to Dr. Gert Goldentops, Architectural Engineering, WPI for developing the first iteration of a flowchart to better understand the International Building Code without his work we would not have been able to complete this project.

Flowchart Rationale

For people not familiar with the International Building Code (IBC), understanding how to navigate its pages can be very difficult. The IBC establishes the minimum regulations for how buildings are constructed. Throughout the code there are specifications based many different things for example, the height of the building, how it be used, how it is built, what the building will be made with, and more. Having to deal with such a wide range of factors results in the IBC being very challenging to follow, this is especially true if one does not already have solid knowledge of the building code.

After analyzing another flowchart aimed at simplifying the IBC, the group decided that the best course of action would be to focus on specialized materials used for exterior wall assemblies. The materials that were selected (Foam Plastic Insulation, High-Pressure Decorative Exterior-Grade Compact Laminates, Fiber-Reinforced Polymer, Exterior Insulation and Finish Systems, Metal Composite Material, and Fire-Retardant Treated Wood) all have distinctive properties that cause them to have unique regulations regarding their usage, as defined in the IBC. While evaluating these different materials, the group noticed that many of them had comparable characteristics and properties.

After exploring ways in which to design the flowchart, the team decided that the properties that overlapped did not provide a solid basis for a singular flowchart which could be used for all of the separate materials. Additionally, referencing the original flowchart, the group agreed that using a different flowchart for each material would provide a much easier to understand and clearer result. While compiling the materials into their own respective flowcharts, the team recognized that many of the materials referenced foam plastic insulation. With the intentions of making everything easy to comprehend, the group decided that making a separate flowchart for foam plastic insulation that could be referenced by the other materials would be helpful. If everything checks out, the flowchart ends with saying that the material is approved for the use. After that whoever is constructing or designing the building must still then pass the usual criteria for the building without having to worry about the unique material restrictions.

While designing the final set of flowcharts the team also generated a guide. The purpose of the guide is to convey how to use the flowchart s. Also, there is a glossary with the different types of construction defined along with the different abbreviations and definitions of many terms used throughout the flowcharts. The guide is a fundamental part in the development of a simplified way to use the IBC, without it understanding the flowchart that was designed may not be any easier to understand.

Using This Report

These flowcharts are designed to make it much easier to use the IBC when designing a building. Many of the complications with the IBC come when trying to use different materials and how they each have their own set of rules and guidelines. Based on this, the next section, where there are flowcharts, are separated by different materials. Just separating the flowcharts by materials would still create a very complicated set of charts. To reduce confusion, the flowcharts are further separated into subcategories based on different conditions regarding how the material would be used. For example, if one was using

High-Pressure Decorative Exterior-Grade Compact Laminates, there are much different stipulations when using them at ground level than when they are used over forty feet in the air.

The directions and contents of the flowcharts will be on the same page. Doing this helps prevent any errors from flipping back and forth or using the wrong directions. On the following page the specific conditions for each different material are listed. These conditions will then point to the corresponding flowchart that should be followed in the next section. Additionally, there is also a glossary describing different materials, building conditions, and common terms from the IBC. The glossary also serves to show the abbreviations used with many terms.

The different materials appear in the following order: Foam Plastic Insulation (FPI), High-Pressure Decorative Exterior-Grade Compact Laminates (HPL), Fiber-Reinforced Polymer (FRP), Exterior Insulation and Finish Systems (EIFS), Metal Composite Material (MCM), and Fire-Retardant Treated Wood (FRT). HPL, FRP, and MCM all contain directions to additionally go through the FPI flowchart. After reaching the box that points to FPI there is no need to go back to that material's flowchart just continue with the FPI chart.

Throughout the flowcharts many rules will state a specific test or standards that the material must meet. Inside the boxes are the section numbers from the IBC. The section numbers will be in parenthesis at the end of the box, while the standards and codes will be in bold to show the distinction between the two numbers.

Material Specific Conditions

Foam Plastic Insulation:

1. Construction Type I-IV – proceed to page 6
2. Construction Type V – proceed to page 7

High-Pressure Decorative Exterior-Grade Compact Laminates:

1. Construction Type I-IV – proceed to page 8
2. Construction Type V – proceed to page 8
3. Installations up to 40 feet in height – proceed to page 9
4. Installations up to 50 feet in height – proceed to page 9

Fiber-Reinforced Polymer Conditions:

1. Construction Type I-V – proceed to page 10
2. Exception 1 – proceed to page 10
3. Exception 2 (Installed on buildings up to 40 feet above the grade) – proceed to page 11

Exterior Insulation and Finish Systems:

1. No specific conditions – proceed to page 12

Metal Composite Material Conditions:

1. Construction Type I-IV – proceed to page 13
2. Construction Type V – proceed to page 13
3. Installations up to 40 feet in height – proceed to page 14
4. Installations up to 50 feet in height – proceed to page 14
5. Installations up to 75 feet in height, Option 1 – proceed to page 15
6. Installations up to 75 feet in height, Option 2 – proceed to page 15
7. Installations over 75 feet – proceed to page 15

Fire-Retardant Treated Wood:

1. No specific conditions – proceed to page 16

Glossary

Construction Types from IBC Chapter 6:

Type I and Type II

Types I and II construction are those types of construction in which the building elements listed in Table 601 are of noncombustible materials, except as permitted in Section 603 and elsewhere in this code.

Type III

Type III construction is that type of construction in which the exterior walls are of noncombustible materials and the interior building elements are of any material permitted by this code. Fire-retardant-treated wood framing complying with Section 2303.2 shall be permitted within exterior wall assemblies of a 2-hour rating or less.

Type IV

Type IV construction (Heavy Timber, HT) is that type of construction in which the exterior walls are of noncombustible materials and the interior building elements are of solid or laminated wood without concealed spaces. The details of Type IV construction shall comply with the provisions of this section. Fire-retardant-treated wood framing complying with Section 2303.2 shall be permitted within exterior wall assemblies with a 2-hour rating or less. Minimum solid sawn nominal dimensions are required for structures built using Type IV construction (HT). For glued laminated members the equivalent net finished width and depths corresponding to the minimum nominal width and depths of solid sawn lumber are required as specified in Table 602.4.

Type V

Type V construction is that type of construction in which the structural elements, exterior walls and interior walls are of any materials permitted by this code.

Abbreviations and Definitions from IBC Chapter 2:

Automatic Sprinkler System = ASS

An automatic sprinkler system, for fire protection purposes, is an integrated system of underground and overhead piping designed in accordance with fire protection engineering standards. The system includes a suitable water supply. The portion of the system above the ground is a network of specially sized or hydraulically designed piping installed in a structure or area, generally overhead, and to which automatic sprinklers are connected in a systematic pattern. The system is usually activated by heat from a fire and discharges water over the fire area.

Exterior Insulation and Finish Systems = EIFS

EIFS are nonstructural, non-load-bearing, exterior wall cladding systems that consist of an insulation board attached either adhesively or mechanically, or both, to the substrate; an integrally reinforced base coat and a textured protective finish coat.

Fiber Reinforced Polymer =FRP

A polymeric composite material consisting of reinforcement fibers, such as glass, impregnated with a fiber-binding polymer which is then molded and hardened. Fiber-reinforced polymers are permitted to contain cores laminated between fiber-reinforced polymer facings.

Fire Resistance Rating

The period of time a building element, component or assembly maintains the ability to confine a fire, continues to perform a given structural function, or both, as determined by the tests, or the methods based on tests, prescribed in Section 703.

Fire-Retardant Treated Wood = FRT

Pressure-treated lumber and plywood that exhibit reduced surface-burning characteristics and resist propagation of fire.

Fire Separation Distance = FSD

The distance measured from the building face to one of the following:

The closest interior lot line

To the centerline of a street, an alley or public way

To an imaginary line between two buildings on the property

The distance shall be measured at right angles from the face of the wall.

Flame Spread Index = FSI

A comparative measure, expressed as a dimensionless number, derived from visual measurements of the spread of flame versus time for a material tested in accordance with ASTM E 84 or UL 723.

Foam Plastic Insulation = FPI

A plastic that is intentionally expanded by the use of a foaming agent to produce a reduced-density plastic containing voids consisting of open or closed cells distributed throughout the plastic for thermal insulating or acoustical purposes and that has a density less than 20 pounds per cubic foot (pcf) (320 kg/m3).

High-Pressure Decorative Exterior-Grade Compact Laminates = HPL

Panels consisting of layers of cellulose fibrous material impregnated with thermosetting resins and bonded together by a high-pressure process to form a homogeneous nonporous core suitable for exterior use.

Metal Composite Material = MCM

A factory manufactured panel consisting of metal skins bonded to both faces of a plastic core.

Smoke Developing Index = SDI

A comparative measure, expressed as a dimensionless number, derived from measurements of smoke obscuration versus time for a material tested in accordance with ASTM E 84 or UL 723.

Foam Plastic Insulation

Foam Plastic Insulation Flowchart 1

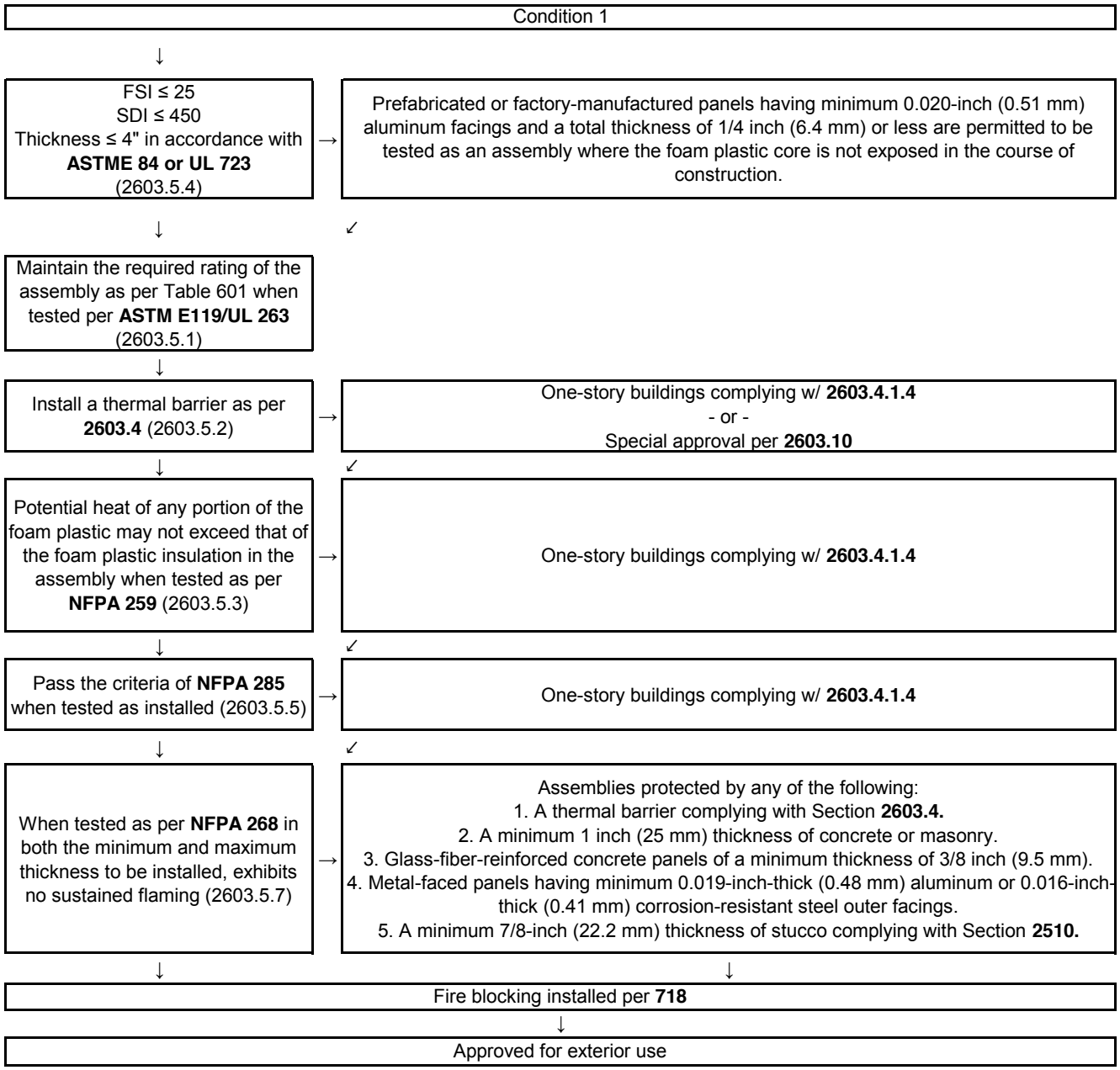

How to use the FPL Flowchart 1:

1. If the criteria in the box is met follow the ↓ symbol down

2. If the criteria in the box is met follow the ↙ symbol to the box down and to the left

3. If the criteria in the box is not met then follow the → symbol to the right

4. If the criteria in the box is not met and there are no symbols then that construction is not permitted

Foam Plastic Insulation Flowchart 2

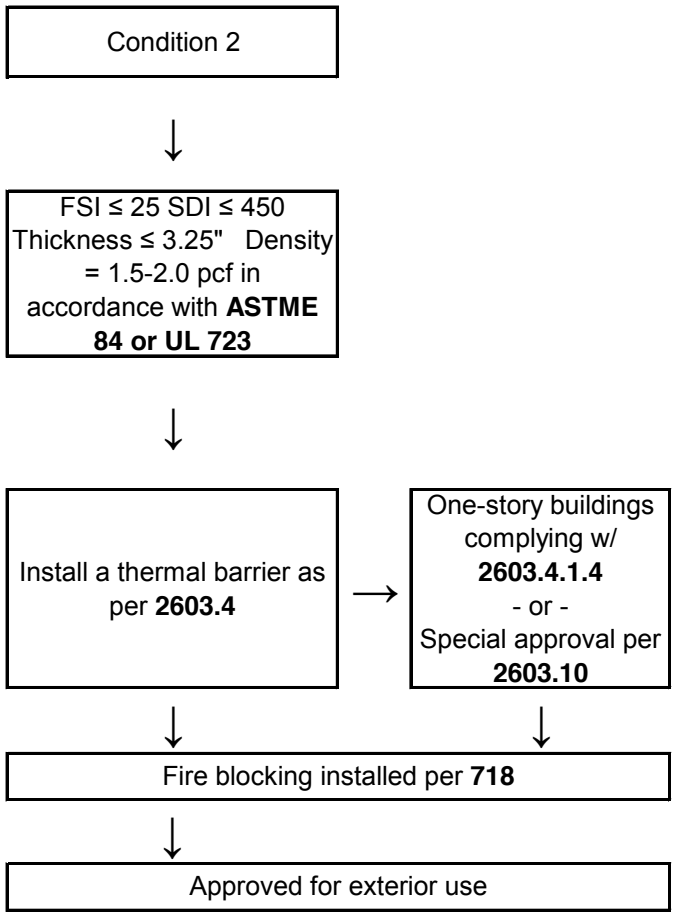

How to use the FPL Flowchart 2 :

1. If the criteria in the box is met follow the ↓ symbol down

2. If the criteria in the box is not met then follow the → symbol to the right

3. If the criteria in the box is not met and there are no symbols then that construction is not permitted

High-Pressure Decorative Exterior-Grade Compact Laminates

High-Pressure Decorative Exterior-Grade Compact Laminates Flowchart 1

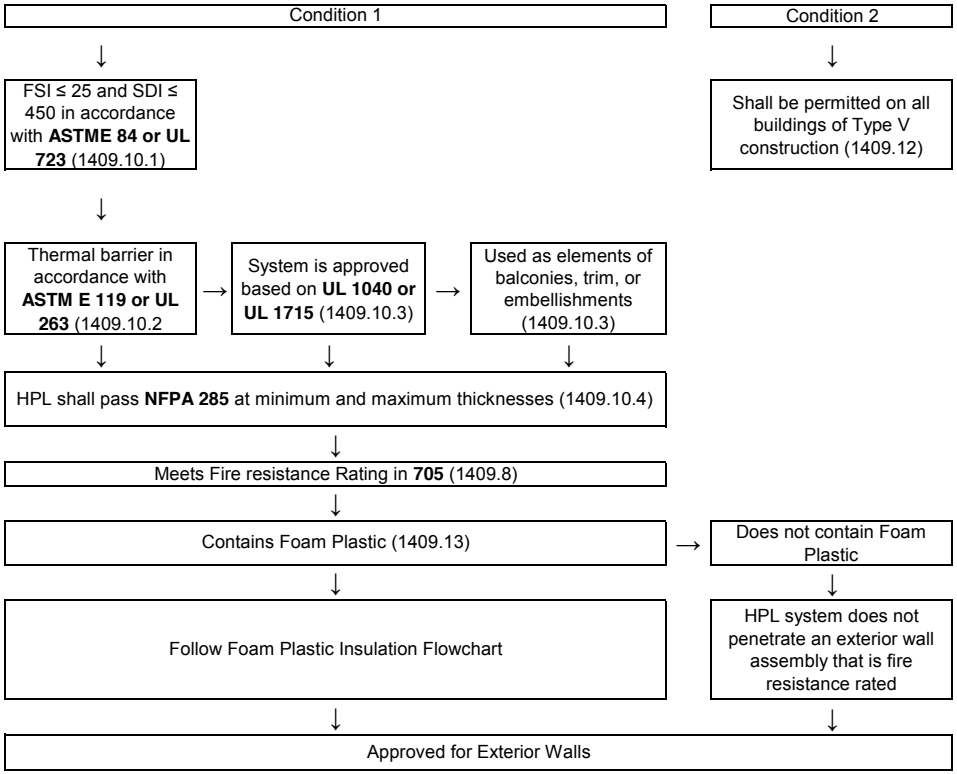

How to use the HPL Flowchart 1:

1. If the criteria in the box is met follow the ↓ symbol down

2. If the criteria in the box is not met then follow the → symbol to the right

3. If the criteria in the box is not met and there are no symbols then that construction is not permitted

High-Pressure Decorative Exterior-Grade Compact Laminates Flowchart 2

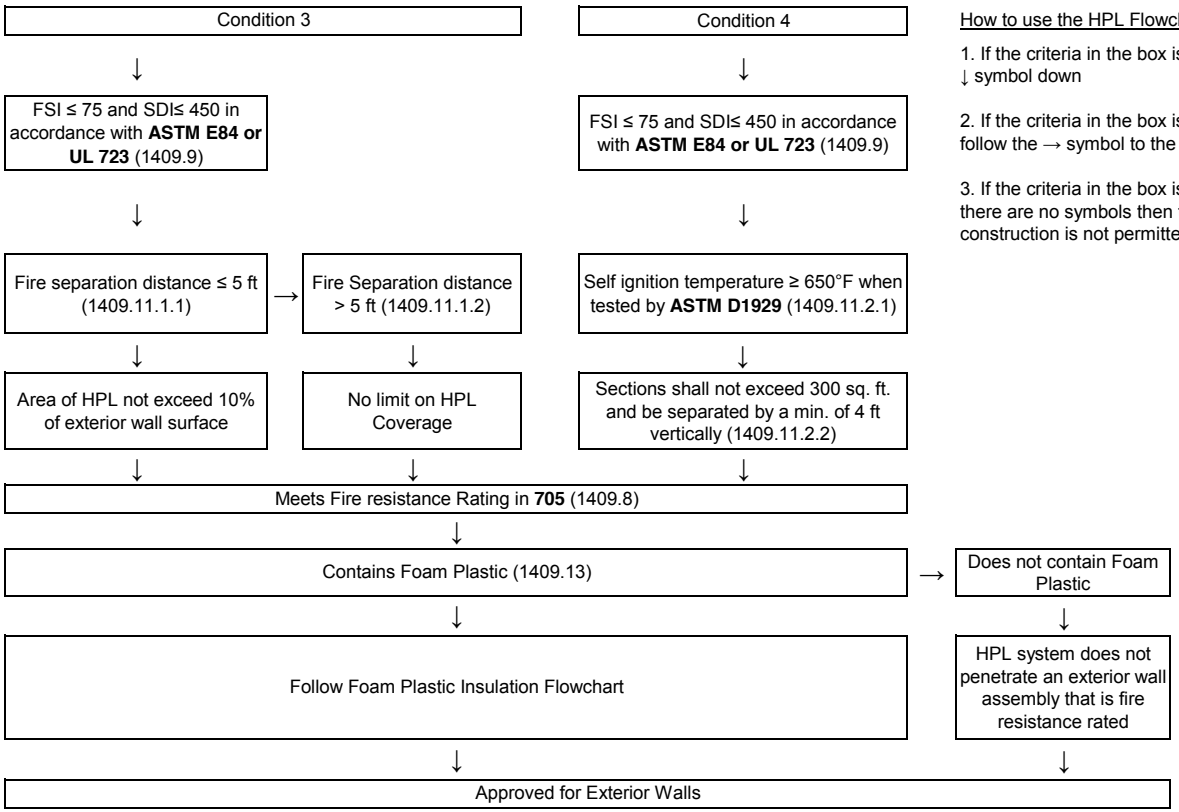

How to use the HPL Flowchart 2:

1. If the criteria in the box is met follow the ↓ symbol down

2. If the criteria in the box is not met then follow the → symbol to the right

3. If the criteria in the box is not met and there are no symbols then that construction is not permitted

Fiber-Reinforced Polymer

Fiber-Reinforced Polymer Flowchart 1

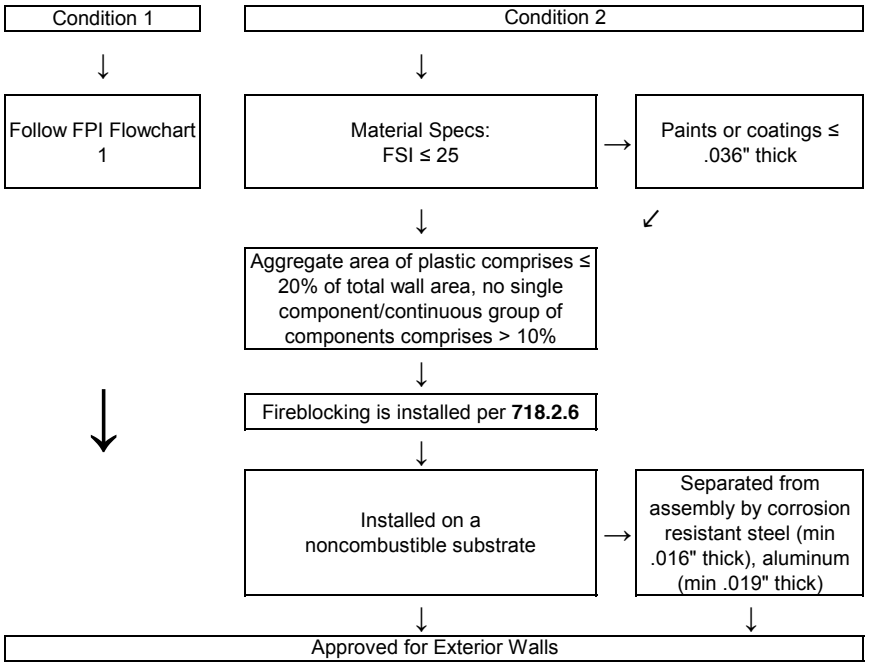

How to use the FRP Flowchart 1:

1. If the criteria in the box is met follow the ↓ symbol down

2. If the criteria in the box is met follow the ↙ symbol to the box down and to the left

3. If the criteria in the box is not met then follow the → symbol right

4. If the criteria in the box is not met and there are no symbols then that construction is not permitted

Fiber-Reinforced Polymer Flowchart 2

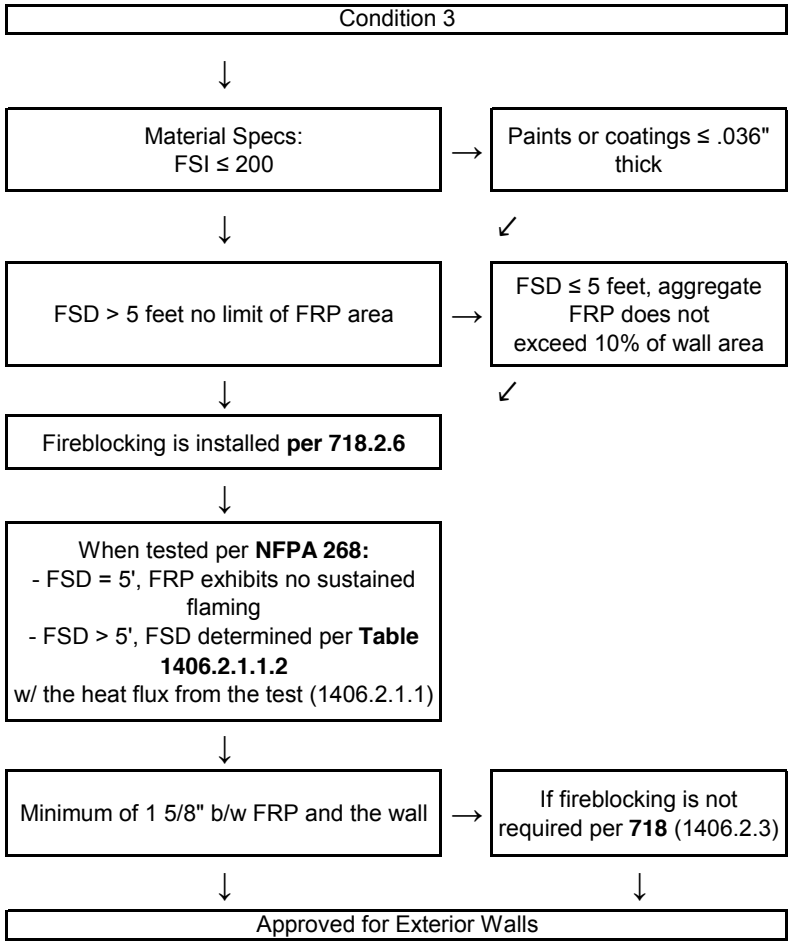

How to use the FRP Flowchart 2:

1. If the criteria in the box is met follow the ↓ symbol down
2. If the criteria in the box is met follow the ↙ symbol to the box down and to the left
3. If the criteria in the box is not met then follow the → symbol right
4. If the criteria in the box is not met and there are no symbols then that construction is not permitted

Exterior Insulation and Finish Systems

Exterior Insulation and Finish Systems FLowchart 1

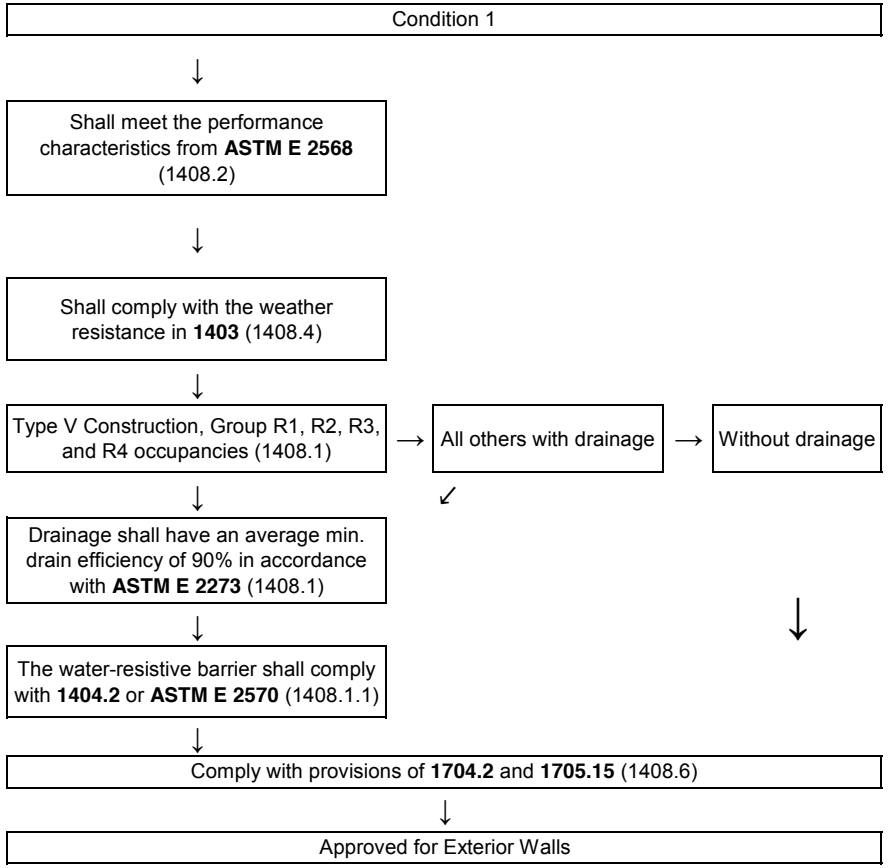

How to use the EIFS Flowchart 1:

1. If the criteria in the box is met follow the ↓ symbol down

2. If the criteria in the box is met follow the ↙ symbol to the box down and to the left

3. If the criteria in the box is not met then follow the → symbol right

4. If the criteria in the box is not met and there are no symbols then that construction is not permitted

Metal Composite Material

Metal Composite Material Flowchart 1

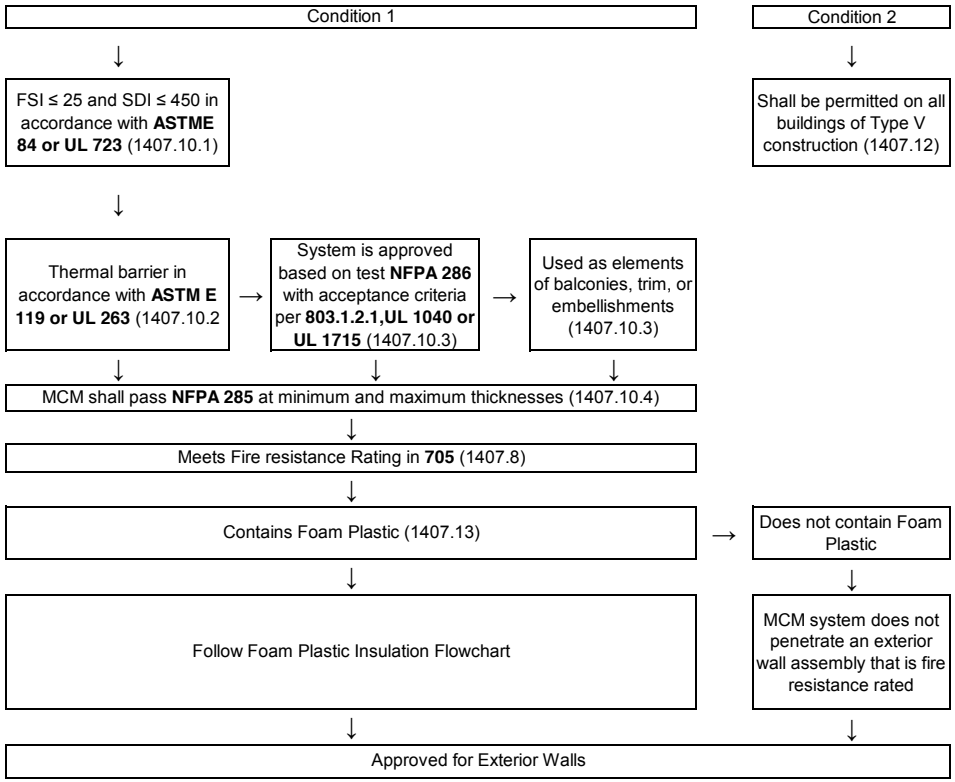

How to use the MCM Flowchart 1:

1. If the criteria in the box is met follow the ↓ symbol down

2. If the criteria in the box is not met then follow the → symbol to the right

3. If the criteria in the box is not met and there are no symbols then that construction is not permitted

Metal Composite Material Flowchart 2

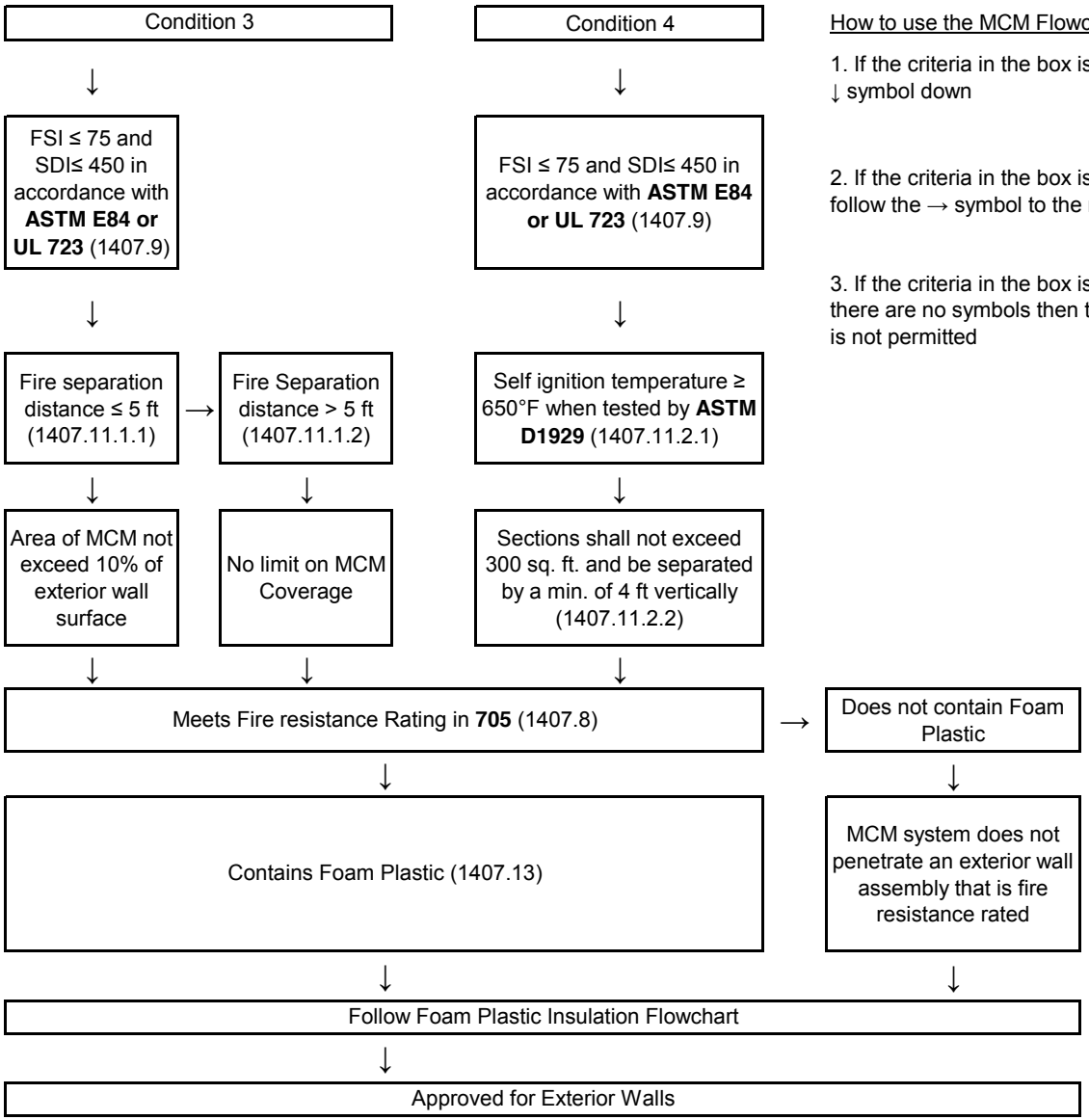

How to use the MCM Flowchart 2:

1. If the criteria in the box is met follow the ↓ symbol down

2. If the criteria in the box is not met then follow the → symbol to the right

3. If the criteria in the box is not met and there are no symbols then that construction is not permitted

Metal Composite Material Flowchart 3

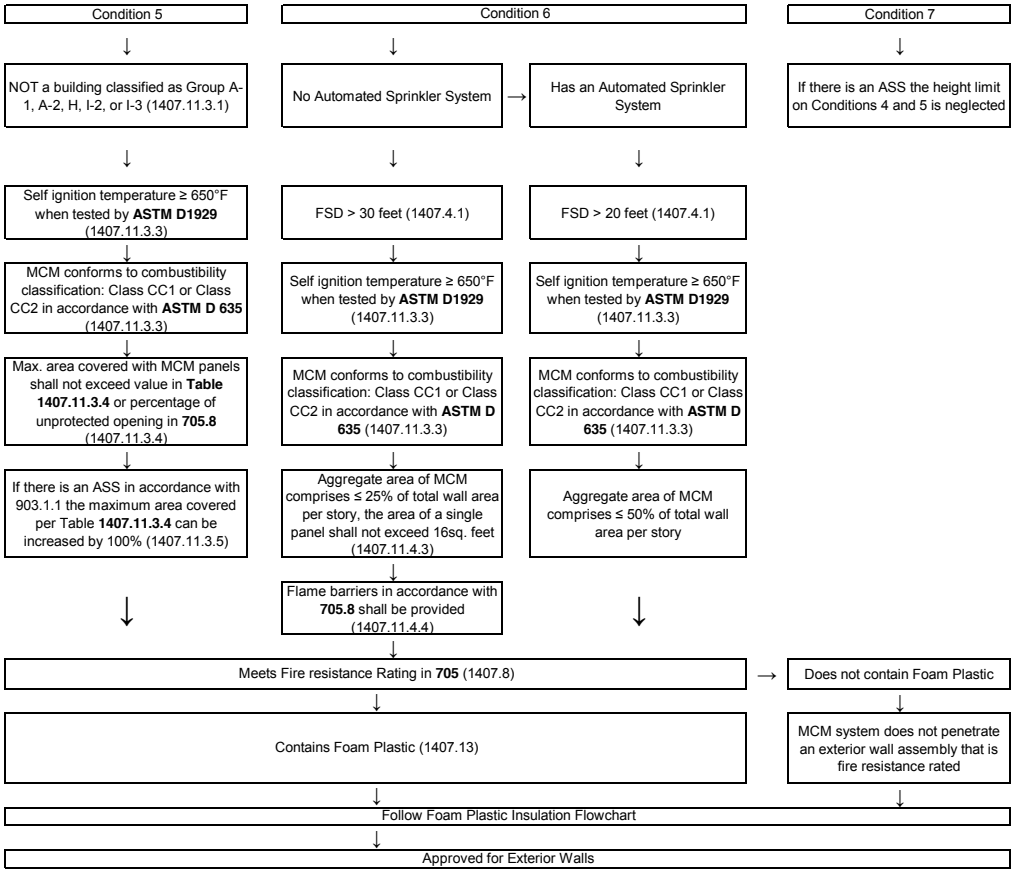

How to use the MCM Flowchart 3:

1. If the criteria in the box is met follow the ↓ symbol down

2. If the criteria in the box is not met then follow the → symbol to the right

3. If the criteria in the box is not met and there are no symbols then that construction is not permitted

Fire-Retardant Treated Wood

Fire-Retardant Treated Wood Flowchart 1

How to use the FRT Flowchart 1:

1. If the criteria in the box is met follow the ↓ symbol down

2. If the criteria in the box is not met then follow the → symbol to the right

3. If the criteria in the box is not met and there are no symbols then that construction is not permitted

Appendix B – Instrumentation

Thermocouple

A thermocouple is an instrument made of two dissimilar metal wires. Type K Thermocouples are the most common type and consist of two wires made from Nickel-Chromium and Nickel-Alumel.[1] On one end, these two wires are fused together to form a junction. When this junction is exposed to a temperature change, a resulting voltage is created. This voltage travels through the wires and is processed by a voltmeter. This voltage is then converted to a temperature using standard equations from the thermocouple manufacturer.[1]

Thermocouples are often used in high thermal insult environments because of their low cost, durability and high temperature limits. Type K Thermocouples have a temperature range of -270C to 1260C with an accuracy of roughly +/-2.2C.[1]

Thin Skin Calorimeters

Thin Skin calorimeters are used to measure incident heat flux on a surface.[2] This instrument is created by welding a thermocouple to the back of a thin metal plate. The thickness of the wire used is dependent on the thickness of the metal plate. The face of the plate is painted black to minimize radiation heat loss. Thin Skin Calorimeters can be calibrated under a known heat flux generated by a cone calorimeter.[2]

The governing equation of the thin skin calorimeter is an energy balance, simplified as:

$$\dot{q}_{storage} = \dot{q}_{in} - \dot{q}_{out}$$

The equation is written explicitly as:

$$\rho c \delta \frac{dT}{dt} = \alpha \dot{q}_i^{"} - \varepsilon\sigma(T_s^4 - T_0^4) - h_{conv}(T_s - T_\infty) - (\varepsilon\sigma T_s^3 + h_{cr})(T_s - T_0)$$

Where the LHS of the equation is the time rate change of energy stored in the plate of the thin skin calorimeter. The first term on the RHS of the equation is the radiative energy absorbed by the plate. The second term is the radiative energy emitted by the plate. The third term is the conductive heat loss from the plate to the environment. And the fourth term is an equation developed by Ris and Khan[3] for calculating the heat loss into the ceramic fiberboard backing. This equation requires the use of a contact resistance, h_{cr}. In order to calculate the contact resistance a transient heat transfer analysis must be completed on a control volume surrounding the plate and its fiberboard backing. An explicit finite difference method is used as a numerical method in order to perform this analysis. An explicit finite difference method uses values at a current time step to evaluate values at a future time, specifically t + dt. A general case is shown below

$$\frac{\partial T}{\partial t} = \frac{T_m^{p+1} - T_m^p}{\Delta t}$$

The boundary condition for the initial node, the node closest to the heated environment is:

$$BC1: -k\frac{\partial T}{\partial y} = h_{cr}(T_r - T_0)$$

Where T_r is the reference temperature from the plate of the thin skin calorimeter and T_0 is the temperature at the initial node 0. The boundary condition for the final node is:

$$BC2: T = T_n$$

Where T_n is the temperature at the final node, n. It should be noted that an additional layer of insulation is added beyond BC2 in order to simplify the solution. This insulation is assumed as perfect. Solving an energy balance at the boundary conditions, plugging in for the general form of an explicit finite difference method, and rearranging results in the following two equations for calculating the surface temperature at the boundary nodes

$$\text{Initial:} \quad T_0^{p+1} = \frac{2\Delta t}{\rho c_p \Delta x} h_{cr}\left(T_r - T_0^p\right) - 2Fo\left(T_0^p - T_1^p\right) + T_0^p$$

$$\text{Final:} \quad T_n^{p+1} = 2Fo\left(T_{n+1}^p - T_n^p\right) + T_0^p$$

Where the subscript n denotes total number of nodes, the subscript p is a point in time, and Fo is the Fourier number

$$Fo = \frac{\alpha \Delta t}{\Delta x^2}$$

Finally for an interior node m, the explicit finite difference solution is:

$$T_m^{p+1} = Fo\left(T_{m+1}^p - 2T_m^p - T_{m-1}^p\right) + T_m^p$$

Additionally it should be noted that an explicit finite difference solution is not unconditionally stable, in that variations in the calculations between time steps could cause a solution to diverge from the correct value. Interior nodes are stable for the condition

$$Fo \leq \frac{1}{2}$$

While a boundary finite difference solution is stable for the condition

$$Fo(1 + Bi) \leq \frac{1}{2}$$

Where Bi is the dimensionless Biot number.

$$Bi = \frac{h\Delta x}{k}$$

Heat Flux Gauges

Heat flux gauges are used to measure net heat flux. The type of heat flux gauge used is specific to the project depending on which form of heat fluxes are primarily being measured. This includes radiative, convective, and conductive heat fluxes. Schmidt-Boelter Gauges are essentially a “uniquely styled thermopile” used to measure mixed heat fluxes.[4] These gauges are often water-cooled which provides a continuous heat sink when the instrument is used in a thermal environment. The minimum sensitivity for a Schmidt-Boelter Gauge is roughly 150 µV/W/cm² with a time response of roughly 500ms.[4]

Bidirectional Probe

A bidirectional probe is a device used to measure flow velocity by utilizing pressure differential through the Bernoulli equation.[5] The probe is similar to a pitot tube with a few changes to make the device more practical for thermal environments. The primary difference between these two instruments is that a bidirectional probe has much larger openings than a pitot tube to prevent soot from becoming entrapped and clogging the device. Another difference is that a bidirectional probe uses insulated pressure transducers to allow for closer use to the fire environment. Also, while many pitot tubes are constructed out of plastics, bidirectional probes are made from metal to prevent melting.[5]

The governing equation of the bidirectional probe is the Bernoulli Equation, shown below:

$$\frac{P_1}{\rho g} + \frac{V_1^2}{2g} + z_1 = \frac{P_2}{\rho g} + \frac{V_2^2}{2g} + z_2$$

For these calculations it is assumed that the density, rho, is that of air at the appropriate temperature, disregarding the effects of the products of combustion on the fluid density. The LHS of the equation is the pressure, velocity and elevation head at an initial location on a streamline. The RHS of the equation is equivalent for a second location on the streamline. For the bidirectional probe, the initial condition is in the environment and the second location is within the chamber of the probe. Because of the design of the probe, the velocity component on the RHS of the equation goes to zero. Due to the experimental setup of the probe, the elevations are constant, and therefore drop out of both sides of the equation. With the above considerations, the velocity of the gas can be found by rearranging to

$$V_1 = \sqrt{\frac{2}{\rho}(P_2 - P_1)}$$

Where P2 comes from the pressure transducer reading from the port of the bidirectional probe.

Appendix C – Exterior Wall Assemblies

The typical components of an exterior wall are shown in Figure 1. These components are exterior cladding (1), drainage planes (2), air barrier systems (3), vapor retarders (4), insulating elements (5), and structural elements (6). These individual elements may both be accomplished by the same material, or be contained individually within the wall system. An example is the use of the exterior layer of a barrier wall as both the exterior cladding and drainage plane.

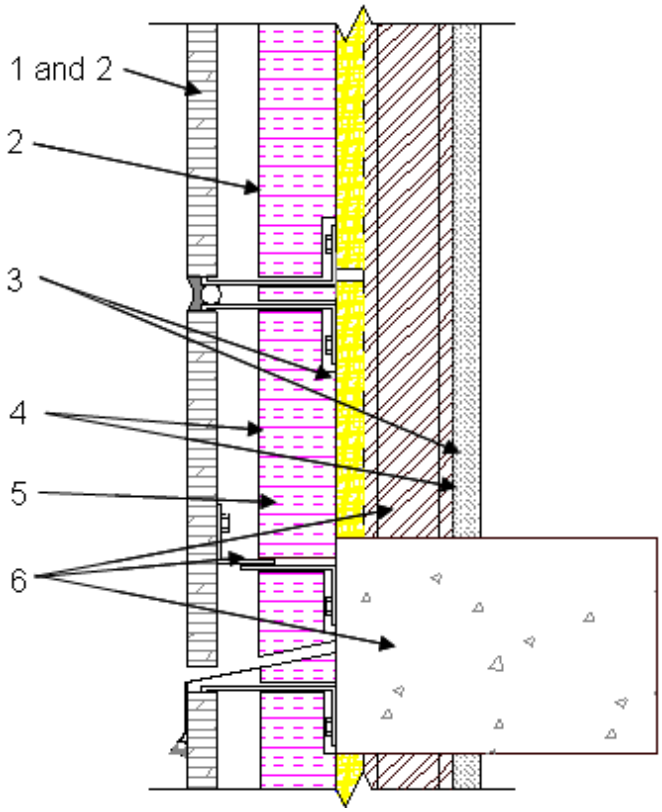

Figure 1 - Typical Exterior Wall Components[6]

Metal Composite Materials (MCM)

The IBC defines Metal Composite Materials as "A factory-manufactured panel consisting of metal skins bonded to both faces of a plastic core." The code establishes general requirements for MCM of a flame spread index of 75 or less and a smoke-developed index of not more than 450 when tested in accordance with ASTM E84 or UL 723. On buildings of Type I-IV construction, the code enforces stricter requirements upon the use of MCM, primarily that the required flame spread index is reduced to 25. Additionally the code requires the use of a thermal barrier separating the MCM from the interior of the building. Finally the IBC requires that any MCM system must pass NFPA 285, when tested as installed with the maximum thickness to be used. Figure 2 shows an example of a typical metal composite material.

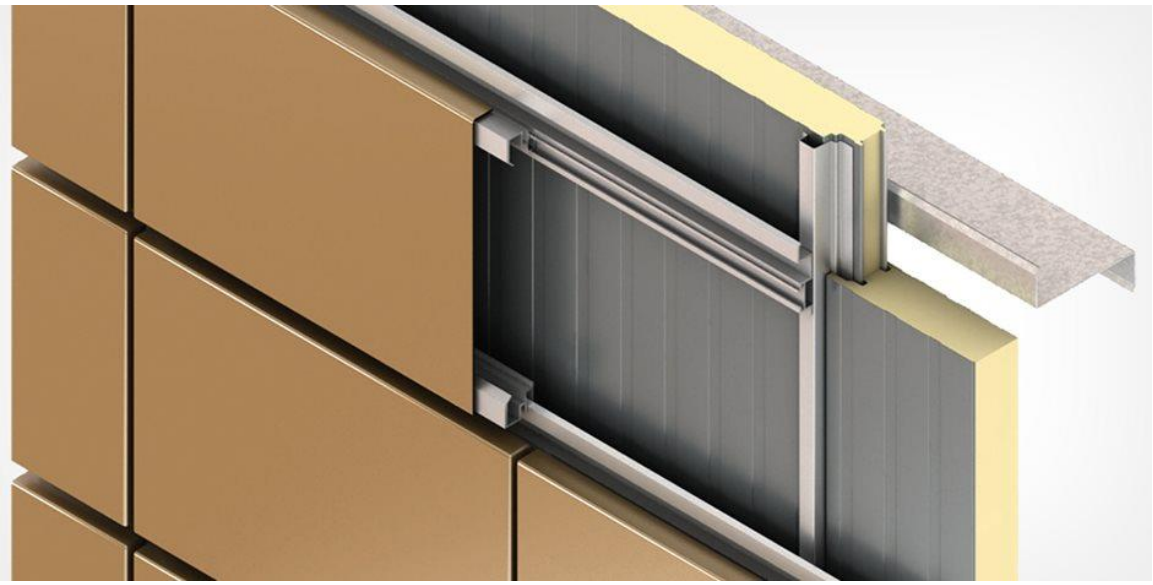

Figure 2 - Example MCM System[7]

Exterior Insulation and Finish Systems (EIFS)

The IBC defines Exterior Insulation and Finish Systems as "nonstructural, nonload-bearing, exterior wall cladding systems that consist of an insulation board attached either adhesively or mechanically, or both, to the substrate; an integrally reinforced base coat and a textured protective finish coat." The code requires the EIFS to comply with ASTM E2568 for performance requirements. Should the EIFS include drainage, it is required to have a drainage efficiency of at least 90 percent. Additionally the code requires that the EIFS adhere to the applicable portions of Chapters 7,14,16,17 and 26. Figure 3 shows an example of an EIFS.

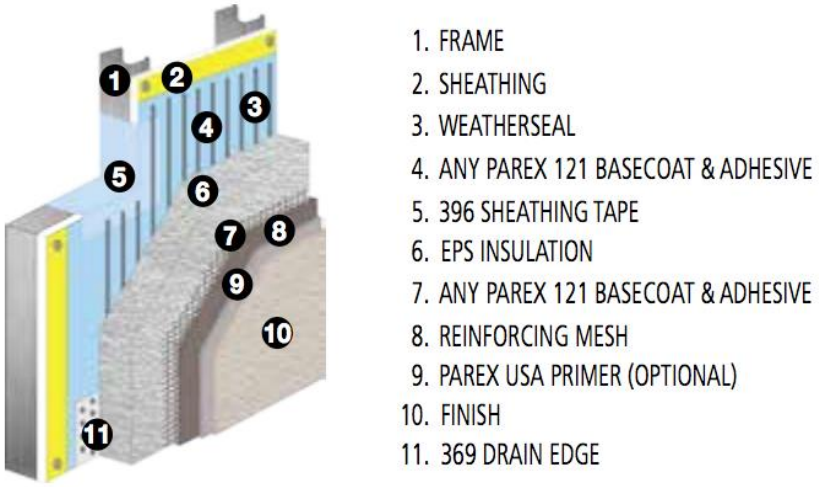

Figure 3 - Example EIFS[8]

High-pressure Decorative Exterior-grade Compact Laminates (HPL)

The IBC defines a High-pressure Decorative Exterior-grade Compact Laminates as "Panels consisting of layers of cellulose fibrous material impregnated with thermosetting resins and bonded together by a high-pressure process to form a homogeneous nonporous core suitable for exterior use." The code

establishes general requirements for HPL similar to that of MCM, requiring a flame spread index of no greater than 75 and a smoke-developed index 450 or less when tested per ASTM E84 or UL 723. For use in Type I-IV construction, the IBC requires a more stringent requirement of a flame spread index of 25. Additionally the IBC specifies that a thermal barrier must be provided to separate the HPL from the interior of the structure. Finally HPL systems are required to pass NFPA 285 in both the minimum and maximum thicknesses to be used. Figure 4 shows an example of an HPL system.

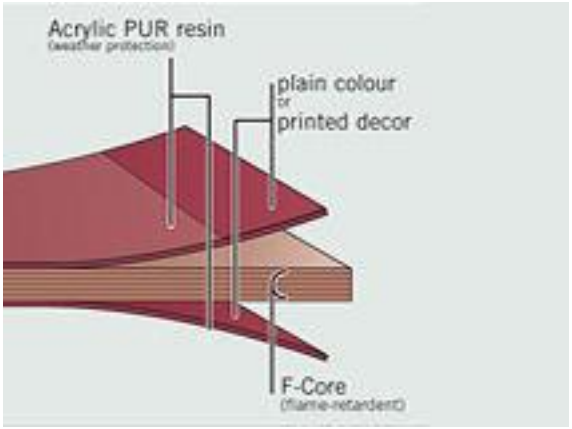

Figure 4 - Example HPL[9]

Appendix D – Heat Transfer Partitioning

Table 1 – Heat Transfer Partitioning of NFPA 285

NFPA 285 - 2 Feet Above Window								
Time Step	Tplume [C]	Twall [C]	q" [kW/m^2]	q"rad [kW/m^2]	% Rad	q"conv [kW/m^2]	% Conv	hc [W/m^2]
0 to 5	359	20	9.00	1.02	11.3%	7.98	88.7%	23.55
5 to 10	546	20	19.00	2.87	15.1%	16.13	84.9%	30.67
10 to 15	605	20	25.00	3.79	15.2%	21.21	84.8%	36.26
15 to 20	639	20	29.00	4.41	15.2%	24.59	84.8%	39.72
20 to 25	674	20	34.00	5.13	15.1%	28.87	84.9%	44.15
25 to 30	702	20	38.00	5.76	15.2%	32.24	84.8%	47.27
NFPA 285 - 3 Feet Above Window								
Time Step	Tplume [C]	Twall [C]	q" [kW/m^2]	q"rad [kW/m^2]	% Rad	q"conv [kW/m^2]	% Conv	hc [W/m^2]
0 to 5	341	20	10.00	0.91	9.1%	9.09	90.9%	28.33
5 to 10	521	20	20.00	2.53	12.7%	17.47	87.3%	34.86
10 to 15	591	20	26.00	3.55	13.7%	22.45	86.3%	39.31
15 to 20	634	20	32.00	4.32	13.5%	27.68	86.5%	45.09
20 to 25	674	20	37.00	5.13	13.9%	31.87	86.1%	48.73
25 to 30	712	20	40.00	6.00	15.0%	34.00	85.0%	49.13
NFPA 285 - 4 Feet Above Window								
Time Step	Tplume [C]	Twall [C]	q" [kW/m^2]	q"rad [kW/m^2]	% Rad	q"conv [kW/m^2]	% Conv	hc [W/m^2]
0 to 5	302	20	8.00	0.70	8.7%	7.30	91.3%	25.90
5 to 10	459	20	15.00	1.83	12.2%	13.17	87.8%	30.00
10 to 15	528	20	20.00	2.63	13.1%	17.37	86.9%	34.20
15 to 20	573	20	25.00	3.27	13.1%	21.73	86.9%	39.30
20 to 25	613	20	30.00	3.93	13.1%	26.07	86.9%	43.96
25 to 30	662	20	34.00	4.87	14.3%	29.13	85.7%	45.37

Table 2 - Heat Transfer Partitioning of Burner

Burner - 2 Feet Above Window								
Time Step	Tplume [C]	Twall [C]	q" [kW/m^2]	q"rad [kW/m^2]	% Rad	q" [kW/m^2]	% Conv	hc [W/m^2]
0 to 5	470	20	17.69	3.26	18.4%	14.44	81.6%	32.08
5 to 10	616	20	31.26	6.66	21.3%	24.61	78.7%	41.32
10 to 15	652	20	33.87	7.82	23.1%	26.05	76.9%	41.22
15 to 20	710	20	36.64	9.96	27.2%	26.69	72.8%	38.71
20 to 25	722	20	40.54	10.45	25.8%	30.09	74.2%	42.89
25 to 30	749	20	43.06	11.64	27.0%	31.43	73.0%	43.13
Burner - 3 Feet Above Window								
Time Step	Tplume [C]	Twall [C]	q" [kW/m^2]	q"rad [kW/m^2]	% Rad	q" [kW/m^2]	% Conv	hc [W/m^2]
0 to 5	366	20	12.52	1.78	14.2%	10.75	85.8%	31.10
5 to 10	550	20	25.94	4.90	18.9%	21.04	81.1%	39.68
10 to 15	613	20	27.48	6.57	23.9%	20.91	76.1%	35.29
15 to 20	694	20	32.19	9.35	29.0%	22.85	71.0%	33.88
20 to 25	723	20	37.01	10.53	28.5%	26.48	71.5%	37.64
25 to 30	745	20	39.71	11.49	28.9%	28.23	71.1%	38.92
Burner - 4 Feet Above Window								
Time Step	Tplume [C]	Twall [C]	q" [kW/m^2]	q"rad [kW/m^2]	% Rad	q" [kW/m^2]	% Conv	hc [W/m^2]
0 to 5	248	20	6.66	0.79	11.8%	5.87	88.2%	25.73
5 to 10	466	20	19.12	3.18	16.6%	15.94	83.4%	35.75
10 to 15	507	20	19.14	3.96	20.7%	15.19	79.3%	31.18
15 to 20	543	20	21.91	4.73	21.6%	17.17	78.4%	32.85
20 to 25	586	20	26.51	5.83	22.0%	20.68	78.0%	36.52
25 to 30	612	20	28.73	6.54	22.8%	22.20	77.2%	37.53

Table 3 - Heat Transfer Partitioning of Kreysler R16

Kreysler R16 Evaluation Test - 2 Feet Above Window								
Time Step	Tplume [K]	Twall [K]	q" [kW/m^2]	q"rad [kW/m^2]	% Rad	q"conv [kW/m^2]	% Conv	hc [W/m^2]
0 to 5	492	303	5.5	0.53	10%	5.0	90%	26.34
5 to 10	705	303	15.2	2.7	18%	12.5	82%	30.93
10 to 15	774	303	21.5	4.2	20%	17.3	80%	36.58
15 to 20	950	303	34.3	8.4	25%	25.9	75%	40.07
20 to 25	1103	303	50.1	15.4	31%	35.6	69%	44.53
25 to 30	1128	303	55.6	16.6	30%	39.3	70%	47.68
Kreysler R16 Evaluation Test - 3 Feet Above Window								
Time Step	Tplume [K]	Twall [K]	q" [kW/m^2]	q"rad [kW/m^2]	% Rad	q"conv [kW/m^2]	% Conv	hc [W/m^2]
0 to 5	472	303	5.3	0.51	10%	4.8	90%	28.47
5 to 10	691	303	16.0	2.4	15%	13.6	85%	35.11
10 to 15	761	303	21.6	3.5	16%	18.11	84%	39.62
15 to 20	863	303	31.1	5.7	18%	25.4	82%	45.43
20 to 25	960	303	41.0	8.8	21%	32.3	79%	49.12
25 to 30	969	303	42.1	9.1	22%	33.0	78%	49.55
Kreysler R16 Evaluation Test - 4 Feet Above Window								
Time Step	Tplume [K]	Twall [K]	q" [kW/m^2]	q"rad [kW/m^2]	% Rad	q"conv [kW/m^2]	% Conv	hc [W/m^2]
0 to 5	449	303	4.23	0.42	10%	3.8	90%	26.0
5 to 10	669	303	13.1	2.1	16%	11.1	84%	30.2
10 to 15	761	303	19.2	3.5	18%	15.6	82%	34.46
15 to 20	863	303	27.9	5.7	20%	22.2	80%	39.59
20 to 25	966	303	38.4	9.0	23%	29.4	77%	44.29
25 to 30	972	303	39.8	9.2	23%	30.6	77%	45.74

Appendix E – Fire Model of NFPA 285

In order to approximate the heat flux experienced by the top of the window frame in NFPA 285, a Fire Dynamics Simulator (FDS) model was constructed and run. Fire modeling a real life situation is a highly variable activity and the best strides were made to construct a model as accurately as possible, however the team recommends that a more comprehensive look into fire modeling NFPA 285 be taken should results from this model be applied more directly than a baseline, order of magnitude approach.

Multiple runs were completed throughout the modeling approach to attempt to determine the best possible settings with which to run the model. A majority of these attempts were attempted at a larger cell size to increase computational efficiency, before reducing the cell size to complete a more accurate run.

The following list summarizes the major differences between the real world NFPA 285 test and the computer model of NFPA 285 completed by the group,

- Compartment dimensions were simplified due to the use of a 0.1m cell size. Dimensions beyond 0.1m in resolution were not possible
- Small floor vents were positioned throughout the burn compartment in an attempt to mix more oxygen in the room as the single window vent was not providing enough oxygen to burn all the fuel released by the burner
- The burners themselves were modeled as basic area burners, keeping the HRRPUA equivalent between NFPA 285 and the model. This was done because the actual burners (cylindrical port in the room and slot in the window) had elements which were sub-grid scale and unable to be refined in this analysis
- All surfaces were defined as nominally concrete, in a calibration run of NFPA 285 the exterior face of the sample is actually gypsum drywall with the paper burned off

The following defines the parameter D* which is suggested by NIST as a validation measure to ensure the cell size of the model is within the range which will provide accurate results.

$$D^* = \left(\frac{\dot{Q}}{c_p \rho_\infty T_\infty \sqrt{g}}\right)^{\frac{2}{5}}$$

NIST suggests a D*/dx value of between 4-16 for valid results. A dx of 0.1m was used in these models.

Window Burner:

Table 4 - Window Burner D*/dx Values

Time Step (min)	HRR (kW)	D*/dx
0 to 5	0	N/A
5 to 10	163	4.6
10 to 15	217	5.2
15 to 20	289	5.8
20 to 25	343	6.2
25 to 30	398	6.6

Room Burner:

Table 5 - Room Burner D*/dx Values

Time Step (min)	HRR (kW)	D*/dx
0 to 5	687	8.3
5 to 10	687	8.3
10 to 15	777	8.7
15 to 20	831	8.9
20 to 25	831	8.9
25 to 30	904	9.3

The following figures display the computational domain of the model as well as a snapshot of the temperature profiles within the model during the test.

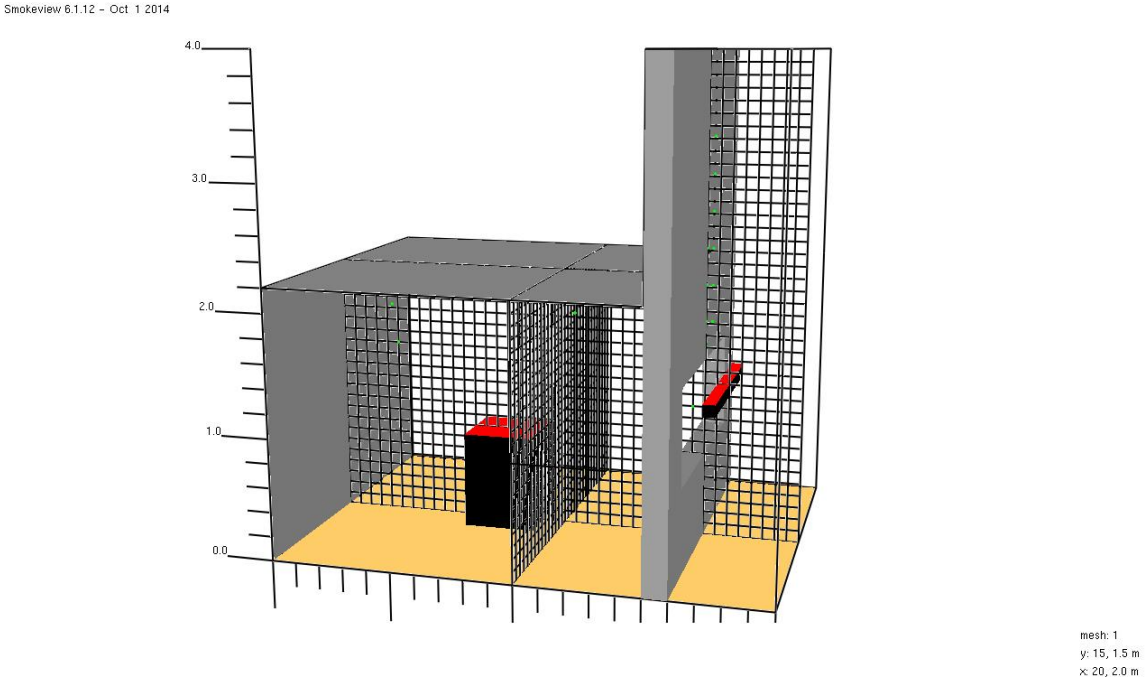

Figure 5 - Computational Domain

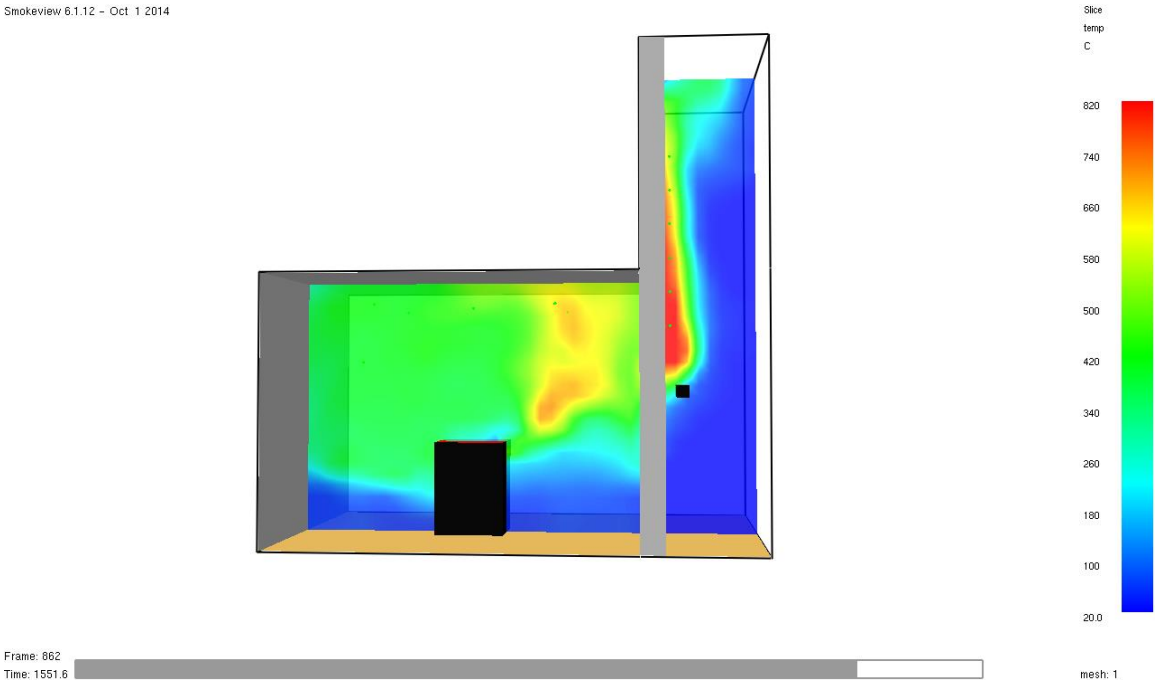

Figure 6 - Sample Temperature Profile

In total the FDS model was able to replicated the plume temperatures and heat fluxes experienced on the exterior of the burn compartment well, with the exception of the lower values experienced by the first instruments which has been termed the entrance effects of the exhaust of the burn compartment. NFPA 285 allows a variance of within 10% of any temperature measurement. This phenomena is thought to be sub-grid scale and unlikely to be resolved in our model.

The following table and figures compare the values provided in a calibration run of NFPA 285 and those simulated by the FDS model.

Table 6 - NFPA 285 vs Model

		0 to 5				5 to 10				10 to 15			
	TC	Cal	High	Low	FDS	Cal	High	Low	FDS	Cal	High	Low	FDS
Ceiling	T18	622	684	560	487	730	803	657	461	806	887	725	541
	T19	622	684	560	525	730	803	657	545	806	887	725	463
	T20	622	684	560	479	730	803	657	436	806	887	725	444
	T21	622	684	560	407	730	803	657	401	806	887	725	447
	T22	622	684	560	422	730	803	657	434	806	887	725	409
Plume	T2	317	349	285	375	466	513	419	582	511	562	460	662
	T3	359	395	323	351	546	601	491	535	605	666	545	604
	T4	341	375	307	323	521	573	469	484	591	650	532	540
	T5	302	332	272	296	459	505	413	437	528	581	475	481
	T6	272	299	245	269	407	448	366	392	469	516	422	426

	T7	244	268	220	243	366	403	329	350	419	461	377	376
	Calorimeter												
Ext. Wall	C2	9	11	7	10.4	19	23	15	24.6	25	30	20	32.3
	C3	10	12	8	8.5	20	24	16	18.9	26	31	21	24.1
	C4	8	6	10	7.1	15	18	12	14.6	20	24	16	18.1
	Sill Flux				17.1				24.6				28

		15 to 20				20 to 25				25 to 30			
	TC	Cal	High	Low	FDS	Cal	High	Low	FDS	Cal	High	Low	FDS
Ceiling	T18	871	958	784	510	869	956	782	482	898	988	808	515
	T19	871	958	784	488	869	956	782	513	898	988	808	478
	T20	871	958	784	452	869	956	782	464	898	988	808	465
	T21	871	958	784	437	869	956	782	427	898	988	808	449
	T22	871	958	784	424	869	956	782	442	898	988	808	425
Plume	T2	533	586	480	768	563	619	507	833	581	639	523	841
	T3	639	703	575	708	674	741	607	774	702	772	632	776
	T4	634	697	571	643	674	741	607	713	712	783	641	703
	T5	573	630	516	580	613	674	552	650	662	728	596	629
	T6	509	560	458	515	542	596	488	581	597	657	537	556
	T7	458	504	412	454	489	538	440	513	543	597	489	487
	Calorimeter												
Ext. Wall	C2	29	35	23	43.7	34	41	27	50.4	38	46	30	52.2
	C3	32	38	26	32.5	37	44	30	37.4	40	48	32	38.2
	C4	25	30	20	25.1	30	36	24	29.4	34	41	37	29.7
	Sill Flux				32.1				34				35.3

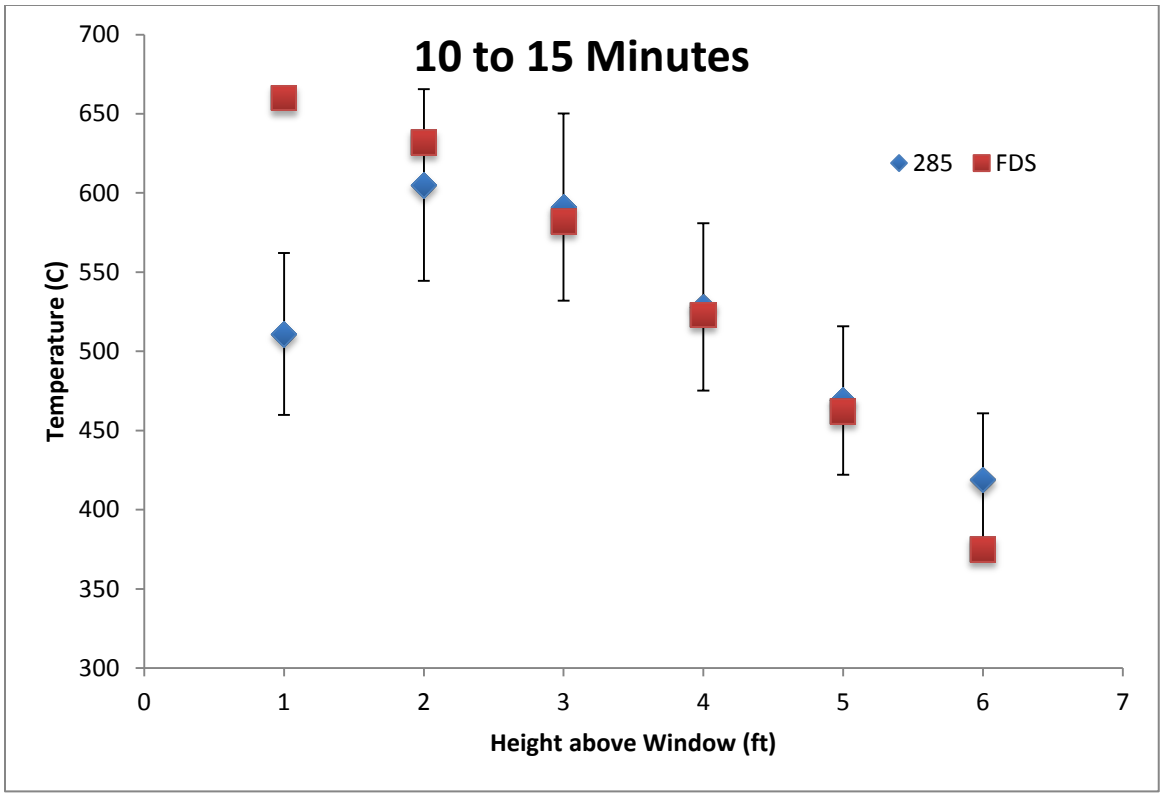

Figure 7 - NFPA vs Model - 10 to 15 min Temperature Profile

The plume temperature was replicated on average 10% off the given values and 5% within if the ignore the first point as sub-grid scale entrance effects. The heat fluxes were replicated to within 15%, which drops to 6% when the entrance effects are again ignored. The interior compartment temperatures however, were only replicated within 41%. The table below summarizes the estimated average heat flux across three points at the bottom of the window frame.

Table 7 - Estimated Window Frame Heat Fluxes

Time Step (min)	Sill Flux (kW/m^2)
0 to 5	17.1
5 to 10	24.6
10 to 15	28
15 to 20	32.1
20 to 25	34
25 to 30	35.3

In order to isolate the issues with the compartment temperatures the model was run again without the window burner and the room burner broken up into 4 equivalent area burners placed centered in the quadrants of the burn compartment. The results are summarized below.

Table 8 - NFPA 285 vs Model (w/out Window Burner)

		0 to 5				5 to 10				10 to 15			
	TC	Cal	High	Low	FDS	Cal	High	Low	FDS	Cal	High	Low	FDS
Ceiling	T18	622	684	560	625	730	803	657	601	806	887	725	602
	T19	622	684	560	644	730	803	657	595	806	887	725	581
	T20	622	684	560	548	730	803	657	546	806	887	725	560
	T21	622	684	560	464	730	803	657	456	806	887	725	461
	T22	622	684	560	456	730	803	657	452	806	887	725	441
Plume	T2	317	349	285	225	466	513	419	246	511	562	460	262
	T3	359	395	323	194	546	601	491	212	605	666	545	226
	T4	341	375	307	168	521	573	469	183	591	650	532	196
	T5	302	332	272	148	459	505	413	161	528	581	475	173
	T6	272	299	245	132	407	448	366	143	469	516	422	154
	T7	244	268	220	120	366	403	329	129	419	461	377	138
	Calorimeter												
Ext. Wall	C2	9	11	7	2.9	19	23	15	3.7	25	30	20	4.2
	C3	10	12	8	2.5	20	24	16	3.2	26	31	21	3.7
	C4	8	6	10	2	15	18	12	2.6	20	24	16	3
	Sill Flux				9.9				11.9				13.2

		15 to 20				20 to 25				25 to 30			
	TC	Cal	High	Low	FDS	Cal	High	Low	FDS	Cal	High	Low	FDS
Ceiling	T18	871	958	784	583	869	956	782	567	898	988	808	571
	T19	871	958	784	550	869	956	782	552	898	988	808	581
	T20	871	958	784	558	869	956	782	550	898	988	808	550
	T21	871	958	784	475	869	956	782	456	898	988	808	439
	T22	871	958	784	437	869	956	782	447	898	988	808	449
Plume	T2	533	586	480	274	563	619	507	286	581	639	523	288
	T3	639	703	575	240	674	741	607	248	702	772	632	248
	T4	634	697	571	209	674	741	607	215	712	783	641	214
	T5	573	630	516	182	613	674	552	188	662	728	596	190
	T6	509	560	458	162	542	596	488	168	597	657	537	171
	T7	458	504	412	147	489	538	440	151	543	597	489	155

	Calorimeter												
Ext. Wall	C2	29	35	23	4.6	34	41	27	5	38	46	30	5
	C3	32	38	26	4.2	37	44	30	4.5	40	48	32	4.5
	C4	25	30	20	3.5	30	36	24	3.9	34	41	37	3.8
	Sill Flux				15.2				17				17.5

The plume temperature was replicated on average 61% off the given values. The heat fluxes were replicated to within 83%. The interior compartment temperatures however, were replicated within 33%. While this is an improvement over the run with the window burner, it is still not within the uncertainty of FDS or the variability allowed by NFPA 285.

In order to then determine the effect of the window burner on the resultant plume, the simulation was run turning the room burner off. The results are shown below.

Table 9 - NFPA 285 vs Model (w/out Room Burner)

	TC	Cal	High	Low	FDS	Cal	High	Low	FDS	Cal	High	Low	FDS
Ceiling	T18	622	684	560	29	730	803	657	45	806	887	725	54
	T19	622	684	560	29	730	803	657	45	806	887	725	52
	T20	622	684	560	29	730	803	657	45	806	887	725	53
	T21	622	684	560	29	730	803	657	45	806	887	725	51
	T22	622	684	560	30	730	803	657	48	806	887	725	58
Plume	T2	317	349	285	209	466	513	419	409	511	562	460	550
	T3	359	395	323	178	546	601	491	356	605	666	545	469
	T4	341	375	307	155	521	573	469	304	591	650	532	396
	T5	302	332	272	137	459	505	413	263	528	581	475	338
	T6	272	299	245	124	407	448	366	230	469	516	422	293
	T7	244	268	220	113	366	403	329	205	419	461	377	258
	Calorimeter												
Ext. Wall	C2	9	11	7	7.2	19	23	15	20.2	25	30	20	33.6
	C3	10	12	8	5.2	20	24	16	13.7	26	31	21	21.9
	C4	8	6	10	4	15	18	12	9.8	20	24	16	14.8
	Sill Flux				3.9				8.6				10.8
		15 to 20				20 to 25				25 to 30			
	TC	Cal	High	Low	FDS	Cal	High	Low	FDS	Cal	High	Low	FDS
Ceiling	T18	871	958	784	65	869	956	782	75	898	988	808	80
	T19	871	958	784	63	869	956	782	73	898	988	808	78

	T20	871	958	784	65	869	956	782	75	898	988	808	79
	T21	871	958	784	65	869	956	782	74	898	988	808	80
	T22	871	958	784	71	869	956	782	82	898	988	808	87
Plume	T2	533	586	480	664	563	619	507	745	581	639	523	788
	T3	639	703	575	561	674	741	607	630	702	772	632	665
	T4	634	697	571	467	674	741	607	522	712	783	641	547
	T5	573	630	516	394	613	674	552	437	662	728	596	454
	T6	509	560	458	337	542	596	488	371	597	657	537	383
	T7	458	504	412	293	489	538	440	321	543	597	489	329
	Calorimeter												
Ext. Wall	C2	29	35	23	46.5	34	41	27	55.9	38	46	30	60.8
	C3	32	38	26	29.5	37	44	30	35.4	40	48	32	38.3
	C4	25	30	20	19.1	30	36	24	22.5	34	41	37	24
	Sill Flux				12.8				14.5				15.4

With the window burner isolated, the plume temperature was replicated on average 33% off the given values, and stays the same when the first thermocouple is discounted. The heat fluxes were replicated to within 30%. The interior compartment temperatures were replicated above 90% variation, which makes sense due to the lack of combustion in the room. Interestingly the heat fluxes to the exterior wall were replicated within 30%, but decreased to 25% once the first calorimeter was discounted. This suggests that the thermal insult received by the wall is due in majority to the presence of the window burner, and not in fact the large compartment burner.

In summary, the models were unable to replicate the interior compartment temperatures of NFPA 285, therefore the window sill heat flux values are valid only for an order of magnitude estimate. This is thought to be due to the geometric layout of the room burner in NFPA 285. Because the room burner is a cylindrical port burner with small ports, it is thought that the fuel leaves the burner at or near jet conditions and entrains a large amount of air not possible to be replicated in these FDS models. However, the model does show strong indications that the plume conditions of NFPA are highly dependent on the presence of the window burner.

References:

NFPA 285: Standard Fire Test Method for Evaluation of Fire Propagation Characteristics of Exterior Non-Load-Bearing Wall Assemblies Containing Combustible Components, 2012

NIST Special Publication 1018: Fire Dynamics Simulator Technical Reference Guide Volume 3: Validation, Sixth Edition

Appendix F – Emissivity of Combustion Products Calculation

The emissivity of the products of methane, propane and butadiene combustion were calculated for use in this report. Methane is used in NFPA 285, propane was used by the group in our burner and butadiene was used as an upper bound on radiation calculations during heat transfer partitioning.

In order to calculate the emissivity of combustion products, both vapors and soot must be considered. The equation for the mixture of combustion gases and soot is as follows:

$$\varepsilon_{total} = (1 - e^{-kS}) + \varepsilon_g e^{-k_s S}$$

Where: S = pathlength (m), assumed to be equivalent to burner slot width

εg = gas emissivity

Ks = effective absorption coefficient of soot (m^-1)

And k is calculated from the following equation, which is valid at the optically thin limit. This is valid due to the controlling nature of the thin flames produced by a slot burner.

$$k = 3.83 \frac{C_0}{C_2} f_v T$$

Where: C2 = Planck's second constant (1.4388E-2 mK)

fv = soot volume fraction

T = Temperature

C0 is a constant based up the index of refraction m = n - ik, and the following formula

$$C_0 = \frac{36\pi nk}{\left(n^2 - k^2 + 2\right)^2 + 4n^2k^2}$$

The emissivity of the gas mixture was calculated using the following equation and the accompanying emissivity charts in the SFPE Handbook.

$$\varepsilon_g = \varepsilon_{H_2O} + \frac{1}{2}\varepsilon_{CO_2}$$

The values for the emissivity's used were averaged across the range of temperatures seen in common fire plumes and flames and NFPA 285, from 600K - 1000K.

The partial pressures of each fuel were used assuming complete combustion of the reactants.

The table below summarizes the inputs of each calculation and the final results of the emissivities.

Table 10 - Emissivity Equation Inputs and Results

	Methane	Propane	Butadiene
C0	4.892196527	4.892196527	4.892196527
n	1.57	1.57	1.57
k	0.56	0.56	0.56
C2 [mK]	1.44E-02	0.014388	0.014388
T [K]	1289	1561	1348

fv	0.00000449	0.00000709	0.0000295
kp (m^-1)	7.537051768	14.41290016	51.78621237
ks (m^-1)	6.45	13.32	45.42
S (m)	0.0127	0.0127	0.0127
e_g	0.023	0.025	0.022
sigma (Wm^-2K^-4)	5.67E-08	5.67E-08	5.67E-08
ep_total	**0.112473141**	**0.188377606**	**0.494307539**

References:

SFPE Handbook, Third Edition, 1-4, 2002

Appendix G – Test Data Burn 1

Table 11 - Test Data Burn 1

Vdot (CFM)			**9**		
HRR' (kW/m)			**467.41**		
Nom. Height (ft)	Height (in)	Height (m)	z/Q'^(2/3)	T [C]	q" (kW/m^2)
1	21	0.53	0.00885629	799.49	46.45
2	33	0.84	0.013917028	829.70	47.80
3	45	1.14	0.018977765	796.86	37.64
4	57	1.45	0.024038502	796.67	27.21
5	69	1.75	0.02909924	722.84	17.72
6	81	2.06	0.034159977	665.00	
7	93	2.36	0.039220715	606.74	
8	105	2.67	0.044281452	551.61	
9	117	2.97	0.049342189	479.61	
Vdot (CFM)			**12**		
HRR' (kW/m)			**623.22**		
Nom. Height (ft)	Height (in)	Height (m)	z/Q'^(2/3)	T [C]	q" (kW/m^2)
1	21	0.53	0.007310707	800.76	47.56
2	33	0.84	0.011488253	876.29	52.27
3	45	1.14	0.0156658	874.57	46.87
4	57	1.45	0.019843347	887.92	38.06
5	69	1.75	0.024020893	859.81	27.51
6	81	2.06	0.02819844	827.16	
7	93	2.36	0.032375987	780.84	
8	105	2.67	0.036553533	719.84	
9	117	2.97	0.04073108	635.29	
Vdot (CFM)			**16**		
HRR' (kW/m)			**830.96**		
Nom. Height (ft)	Height (in)	Height (m)	z/Q'^(2/3)	T [C]	q" (kW/m^2)
1	21	0.53	0.006034855	796.15	48.88
2	33	0.84	0.009483344	866.80	55.86
3	45	1.14	0.012931833	883.20	54.14
4	57	1.45	0.016380322	893.35	45.98
5	69	1.75	0.01982881	887.24	36.73
6	81	2.06	0.023277299	873.16	
7	93	2.36	0.026725788	845.90	
8	105	2.67	0.030174277	812.58	
9	117	2.97	0.033622766	743.18	
Vdot (CFM)			**19**		

HRR' (kW/m)			**986.76**		
Nom. Height (ft)	Height (in)	Height (m)	z/Q'^(2/3)	T [C]	q" (kW/m^2)
1	21	0.53	0.005381596	794.28	49.54
2	33	0.84	0.008456794	860.48	60.22
3	45	1.14	0.011531992	879.35	57.98
4	57	1.45	0.01460719	890.51	50.30
5	69	1.75	0.017682388	897.15	43.12
6	81	2.06	0.020757586	887.50	
7	93	2.36	0.023832784	865.16	
8	105	2.67	0.026907982	845.99	
9	117	2.97	0.02998318	790.48	
Vdot (CFM)			**22**		
HRR' (kW/m)			**1142.57**		
Nom. Height (ft)	Height (in)	Height (m)	z/Q'^(2/3)	T [C]	q" (kW/m^2)
1	21	0.53	0.004880508	808.08	52.17
2	33	0.84	0.00766937	868.50	69.84
3	45	1.14	0.010458232	877.73	62.78
4	57	1.45	0.013247094	899.51	55.57
5	69	1.75	0.016035956	906.01	48.52
6	81	2.06	0.018824818	894.18	
7	93	2.36	0.02161368	874.00	
8	105	2.67	0.024402542	866.65	
9	117	2.97	0.027191404	826.41	

Appendix H – Test Data Burn 2

Table 12 - Test Data Burn 2

Vdot (CFM)			**1**			**1.5**			**2**			**2.5**		
HRR' (kW/m)			**51.93**			**77.90**			**103.87**			**129.84**		
Nom. Height (ft)	Height (in)	Height (m)	z/Q'^ (2/3)	T [C]	q" (kW/m^2)	z/Q'^ (2/3)	T [C]	q" (kW/m^2)	z/Q'^ (2/3)	T [C]	q" (kW/m^2)	z/Q'^ (2/3)	T [C]	q" (kW/m^2)
1	21	0.5334	0.038	42.83	0.18	0.029	173.95	2.46	0.024	215.77	3.46	0.021	252	6.54
2	33	0.8382	0.060	32.67	0.04	0.046	109.77	1.83	0.038	131.23	2.69	0.033	151.66	3.25
3	45	1.143	0.082	26.11	0.17	0.063	80.41	1.72	0.052	92.24	2.21	0.045	105.56	2.43
4	57	1.4478	0.104	23.14	0.01	0.079		0.98	0.066		1.27	0.056		1.44
5	69	1.7526	0.126	20.75	-0.03	0.096	54.22	0.65	0.079	59.37	0.81	0.068	65.96	1.00
6	81	2.0574	0.148	18.93	-0.05	0.113	45	0.54	0.093	49.9	0.69	0.080	56.29	0.85
7	93	2.3622	0.170	17.94		0.130	39.07		0.107	42.87		0.092	48.68	
8	105	2.667	0.192	17.58		0.146	35.84		0.121	39.52		0.104	44.47	
Vdot (CFM)			**3**			**3.5**			**4**			**4.5**		
HRR' (kW/m)			**155.80**			**181.77**			**207.74**			**233.71**		
Nom. Height (ft)	Height (in)	Height (m)	z/Q'^ (2/3)	T [C]	q" (kW/m^2)	z/Q'^ (2/3)	T [C]	q" (kW/m^2)	z/Q'^ (2/3)	T [C]	q" (kW/m^2)	z/Q'^ (2/3)	T [C]	q" (kW/m^2)
1	21	0.5334	0.018	329.55	12.05	0.017	360.81	11.30	0.015	398.76	6.52	0.014	439.15	10.75
2	33	0.8382	0.029	192	4.33	0.026	218.47	5.43	0.024	239.93	6.26	0.022	292.69	8.60
3	45	1.143	0.039	131.57	3.22	0.036	141.79	3.52	0.033	165.03	4.05	0.030		5.37
4	57	1.4478	0.050		1.90	0.045		2.02	0.041		2.27	0.038		2.96
5	69	1.7526	0.061	76.92	1.27	0.055	80.9	1.40	0.050	91.54	1.61	0.046	111.41	2.05
6	81	2.0574	0.071	63.28	1.03	0.064	66.93	1.14	0.059	73.77	1.26	0.054	90.49	1.68

7	93	2.3622	0.082	52.97		0.074	57.34		0.067	61.81		0.062	74.76	
8	105	2.667	0.092	47.26		0.083	52.01		0.076	55.62		0.070	67.34	
Vdot (CFM)			**5**			**5.5**			**6**			**6.5**		
HRR' (kW/m)			**259.67**			**285.64**			**311.61**			**337.58**		
Nom. Height (ft)	Height (in)	Height (m)	z/Q'^ (2/3)	T [C]	q" (kW/m^2)	z/Q'^ (2/3)	T [C]	q" (kW/m^2)	z/Q'^ (2/3)	T [C]	q" (kW/m^2)	z/Q'^ (2/3)	T [C]	q" (kW/m^2)
1	21	0.5334	0.013	550.46	14.61	0.012	589.65	16.71	0.012	587.35	18.21	0.011	635.78	20.59
2	33	0.8382	0.021	375.39	12.36	0.019	407.24	13.67	0.018	409.3	15.60	0.017	457.53	17.61
3	45	1.143	0.028		7.15	0.026		7.78	0.025	348.61	8.52	0.024	338.35	9.47
4	57	1.4478	0.036		3.83	0.033	356.9	3.99	0.031	309.37	4.35	0.030	307.63	4.83
5	69	1.7526	0.043	138.02	2.64	0.040	138.94	2.67	0.038	145.53	2.92	0.036	162.8	3.14
6	81	2.0574	0.051	110.68	2.15	0.047	107.39	2.00	0.045	114.7	2.24	0.042	125.57	2.38
7	93	2.3622	0.058	89.4		0.054	85.43		0.051	92.09		0.049	97.92	
8	105	2.667	0.066	79.1		0.061	75.08		0.058	80.87		0.055	84.62	
Vdot (CFM)			**7**			**7.5**			**8**			**8.5**		
HRR' (kW/m)			**363.54**			**389.51**			**415.48**			**441.45**		
Nom. Height (ft)	Height (in)	Height (m)	z/Q'^ (2/3)	T [C]	q" (kW/m^2)	z/Q'^ (2/3)	T [C]	q" (kW/m^2)	z/Q'^ (2/3)	T [C]	q" (kW/m^2)	z/Q'^ (2/3)	T [C]	q" (kW/m^2)
1	21	0.5334	0.010	659.69	21.68	0.010	620.89	21.15	0.010	609.02	21.37	0.009	739.82	23.98
2	33	0.8382	0.016	479.02	19.75	0.016	456.85	18.25	0.015	453.18	17.78	0.014	561.91	25.78
3	45	1.143	0.022	353.09	11.53	0.021	338.51	10.19	0.021	332.47	9.71	0.020	426.08	15.58
4	57	1.4478	0.028	307.99	5.57	0.027	271.22	5.32	0.026	254.02	5.06	0.025	329.27	7.62
5	69	1.7526	0.034	176.78	3.67	0.033	179.74	3.71	0.031	166.69	2.54	0.030	219.44	4.80
6	81	2.0574	0.040	138.39	2.79	0.039	137.92	2.74	0.037	130.96	2.54	0.035	165.1	3.43
7	93	2.3622	0.046	108.43		0.044	108.05		0.042	105.77		0.041	126.74	

8	105	2.667	0.052	94.06		0.050	94.23		0.048	93.44		0.046	109.6	
Vdot (CFM)			**9**			**9.5**			**10**			**10.5**		
HRR' (kW/m)			**467.41**			**493.38**			**519.35**			**545.32**		
Nom. Height (ft)	Height (in)	Height (m)	z/Q'^ (2/3)	T [C]	q" (kW/m^2)	z/Q'^ (2/3)	T [C]	q" (kW/m^2)	z/Q'^(2/3)	T [C]	q" (kW/m^2)	z/Q'^ (2/3)	T [C]	q" (kW/m^2)
1	21	0.5334	0.009	622.47	22.60	0.009	699.11	23.74	0.008	682.86	24.21	0.008	740.7	25.67
2	33	0.8382	0.014	461.68	19.55	0.013	542.29	23.78	0.013	528.25	22.59	0.013	595.38	27.01
3	45	1.143	0.019	347.32	10.94	0.018	417.26	14.73	0.018	394.33	13.51	0.017	452.76	16.96
4	57	1.4478	0.024	275.4	5.78	0.023	323.8	7.46	0.022	315.26	7.54	0.022	360.36	8.74
5	69	1.7526	0.029	179.56	3.93	0.028	215.89	4.72	0.027	216.06	5.00	0.026	247.07	5.62
6	81	2.0574	0.034	141.94	2.86	0.033	162.87	3.27	0.032	164.75	3.43	0.031	190.66	3.89
7	93	2.3622	0.039	113.52		0.038	125.21		0.037	126.37		0.035	144.97	
8	105	2.667	0.044	97.18		0.043	108.65		0.041	107.4		0.040	123.51	

Appendix I – Test Data Burn 3

Table 13 - Test Data Burn 3

Vdot (CFM)			**2.43**		
HRR' (kW/m)			**126.20**		
Nom. Height (ft)	Height (in)	Height (ft)	z/Q'^(2/3)	T [C]	q" (kW/m^2)
1	21	0.5334	0.021200332	343.9284976	3.949643614
2	33	0.8382	0.033314808	201.1185414	4.633145604
3	45	1.143	0.045429284	147.9061374	3.928532859
4	57	1.4478	0.05754376	107.7146274	2.309026483
5	69	1.7526	0.069658235	86.40142447	1.562915467
6	81	2.0574	0.081772711	73.11964743	1.379654698
7	93	2.3622	0.093887187	62.49281184	
8	105	2.667	0.106001662	58.17483728	
Vdot (CFM)			**3.24**		
HRR' (kW/m)			**168.27**		
Nom. Height (ft)	Height (in)	Height (ft)	z/Q'^(2/3)	T [C]	q" (kW/m^2)
1	21	0.5334	0.017500489	421.5780011	6.608478148
2	33	0.8382	0.027500768	258.2286562	6.744328749
3	45	1.143	0.037501048	178.7966895	4.65668759
4	57	1.4478	0.047501327	128.2653624	2.767063779
5	69	1.7526	0.057501606	100.0152335	1.950600616
6	81	2.0574	0.067501886	82.34214846	1.632420056
7	93	2.3622	0.077502165	70.22034319	
8	105	2.667	0.087502444	64.45947893	
Vdot (CFM)			**4.31**		
HRR' (kW/m)			**223.84**		
Nom. Height (ft)	Height (in)	Height (ft)	z/Q'^(2/3)	T [C]	q" (kW/m^2)
1	21	0.5334	0.014468672	432.1923472	8.271867989
2	33	0.8382	0.022736485	289.123489	8.070909062
3	45	1.143	0.031004297	200.1744713	5.372339287
4	57	1.4478	0.03927211	140.6422545	3.12591741
5	69	1.7526	0.047539923	109.4334065	2.161854259
6	81	2.0574	0.055807735	91.12838595	1.787868543
7	93	2.3622	0.064075548	77.04199942	
8	105	2.667	0.07234336	71.60220403	
Vdot (CFM)			**5.12**		
HRR' (kW/m)			**265.91**		
Nom. Height (ft)	Height (in)	Height (ft)	z/Q'^(2/3)	T [C]	q" (kW/m^2)
1	21	0.5334	0.012899322	559.978304	11.01370825
2	33	0.8382	0.020270363	385.4123912	12.20686809
3	45	1.143	0.027641404	265.7135256	7.218805216

4	57	1.4478	0.035012445	179.3518716	4.054622597
5	69	1.7526	0.042383486	135.7052912	2.789372161
6	81	2.0574	0.049754527	110.3724927	2.240435177
7	93	2.3622	0.057125568	91.09491509	
8	105	2.667	0.064496609	81.11659017	
Vdot (CFM)			**5.94**		
HRR' (kW/m)			**308.49**		
Nom. Height (ft)	Height (in)	Height (ft)	z/Q'^(2/3)	T [C]	q" (kW/m^2)
1	21	0.5334	0.011683041	547.7029825	11.87243162
2	33	0.8382	0.018359064	366.3689478	12.01737967
3	45	1.143	0.025035087	260.5353001	6.611873046
4	57	1.4478	0.031711111	175.8463305	3.748887176
5	69	1.7526	0.038387134	133.6257111	2.696474195
6	81	2.0574	0.045063157	106.4206538	2.085555165
7	93	2.3622	0.05173918	86.48769647	
8	105	2.667	0.058415204	77.15530296	

Appendix J – Test Data Burn 4

Table 14 - Test Data Burn 4

Vdot (CFM)			**4.77**		
HRR' (kW/m)			**247.50**		
Nominal Height	Height	Height (m)	z/Q'^(2/3)	T [C]	q" (kW/m^2)
1	21	0.5334	0.013531352	603.24	9.98
2	33	0.8382	0.021263554	470.09	17.70
3	45	1.143	0.028995755	365.61	12.53
4	57	1.4478	0.036727957	248.22	6.66
5	69	1.7526	0.044460158	184.49	4.35
6	81	2.0574	0.052192359	144.16	3.52
7	93	2.3622	0.059924561	113.04	
8	105	2.667	0.067656762	98.19	
Vdot (CFM)			**9.6**		
HRR' (kW/m)			**498.6580623**		
Nominal Height	Height	Height (m)	z/Q'^(2/3)	T [C]	q" (kW/m^2)
1	21	0.5334	0.008482381	749.8970798	15.51736115
2	33	0.8382	0.013329456	695.2021086	35.02241379
3	45	1.143	0.018176531	639.8786275	30.65443063
4	57	1.4478	0.023023606	496.0831343	19.50269432
5	69	1.7526	0.027870681	394.1300255	13.47151087
6	81	2.0574	0.032717756	308.1432669	9.275297815
7	93	2.3622	0.037564831	225.4471718	
8	105	2.667	0.042411906	185.676629	
Vdot (CFM)			**11.97**		
HRR' (kW/m)			**621.4892762**		
Nominal Height	Height	Height (m)	z/Q'^(2/3)	T [C]	q" (kW/m^2)
1	21	0.5334	0.007324263	773.3724486	16.62461833
2	33	0.8382	0.011509556	709.599636	36.64911033
3	45	1.143	0.015694849	694.3508316	32.19897693
4	57	1.4478	0.019880142	542.806996	21.905385
5	69	1.7526	0.024065435	435.2589302	15.72834934
6	81	2.0574	0.028250728	354.4745911	10.92299716
7	93	2.3622	0.032436021	265.3482464	
8	105	2.667	0.036621314	214.398565	
Vdot (CFM)			**13.63**		
HRR' (kW/m)			**707.654456**		
Nominal Height	Height	Height (m)	z/Q'^(2/3)	T [C]	q" (kW/m^2)
1	21	0.5334	0.006716951	768.2277092	18.11016343
2	33	0.8382	0.010555209	721.5368883	40.54115127
3	45	1.143	0.014393466	723.4259649	37.00882678

4	57	1.4478	0.018231724	586.3546204	26.50709225
5	69	1.7526	0.022069982	486.5044058	19.40455974
6	81	2.0574	0.02590824	399.0346558	12.88954327
7	93	2.3622	0.029746497	291.5544858	
8	105	2.667	0.033584755	235.0853955	
Vdot (CFM)			**15.11**		
HRR' (kW/m)			**784.6531274**		
Nominal Height	Height	Height (m)	z/Q'^(2/3)	T [C]	q" (kW/m^2)
1	21	0.5334	0.006270005	779.8265029	19.74824985
2	33	0.8382	0.009852865	748.6690802	43.06550887
3	45	1.143	0.013435725	745.3232221	39.71316492
4	57	1.4478	0.017018584	611.5312421	28.73933052
5	69	1.7526	0.020601444	509.1321155	21.89777567
6	81	2.0574	0.024184304	426.4296871	14.82916399
7	93	2.3622	0.027767164	323.3587367	
8	105	2.667	0.031350024	260.5721736	
Vdot (CFM)			**17.26**		
HRR' (kW/m)			**896.4845311**		
Nominal Height	Height	Height (m)	z/Q'^(2/3)	T [C]	q" (kW/m^2)
1	21	0.5334	0.005737083	782.8355632	20.28250626
2	33	0.8382	0.009015416	737.0154135	44.05218239
3	45	1.143	0.01229375	744.1071754	41.39020804
4	57	1.4478	0.015572083	615.5720055	30.66553647
5	69	1.7526	0.018850416	521.0464093	24.16756538
6	81	2.0574	0.022128749	457.4692816	17.06450703
7	93	2.3622	0.025407083	352.4422323	
8	105	2.667	0.028685416	284.8478061	

Appendix K – Test Data Burn 5

Table 15 - Test Data Burn 5

Vdot (CFM)			**6**		
HRR' (kW/m)			**311.61**		
Nominal Height	Height	**Height (m)**	z/Q'^(2/3)	T [C]	q" (kW/m^2)
1	21	0.5334	0.000155377	683.0612441	
2	33	0.8382	0.000170594	615.5628697	31.26614491
3	45	1.143	0.000173352	550.1407719	25.9408737
4	57	1.4478	0.000190182	465.9386275	19.12869319
5	69	1.7526	0.000211878	372.8740109	14.08849899
6	81	2.0574	0.000226219	284.64	
7	93	2.3622	0.000232628	215.2978868	
8	105	2.667	0.000259339	177.5251224	
Vdot (CFM)			**7.4**		
HRR' (kW/m)			**384.3182033**		
Nominal Height	Height	**Height (m)**	z/Q'^(2/3)	T [C]	q" (kW/m^2)
1	21	0.5334	0.010090803	689.3621316	
2	33	0.8382	0.015856975	651.9927053	33.8731072
3	45	1.143	0.021623148	612.5651258	27.48270066
4	57	1.4478	0.027389321	507.0751659	19.14320029
5	69	1.7526	0.033155494	373.9557539	12.8963285
6	81	2.0574	0.038921667	290.4423436	8.23693823
7	93	2.3622	0.04468784	221.8112015	
8	105	2.667	0.050454013	184.7935518	
Vdot (CFM)			**9.6**		
HRR' (kW/m)			**498.5749665**		
Nominal Height	Height	**Height (m)**	z/Q'^(2/3)	T [C]	q" (kW/m^2)
1	21	0.5334	0.008483324	730.853759	
2	33	0.8382	0.013330937	709.8208964	40.81661292
3	45	1.143	0.018178551	704.129395	37.13360699
4	57	1.4478	0.023026164	611.3110934	27.54765527
5	69	1.7526	0.027873777	476.7511485	19.88420429
6	81	2.0574	0.032721391	391.6408989	13.08435755
7	93	2.3622	0.037569004	298.5330497	
8	105	2.667	0.042416618	238.8580212	
Vdot (CFM)			**11.3**		
HRR' (kW/m)			**586.8642834**		
Nominal Height	Height	**Height (m)**	z/Q'^(2/3)	T [C]	q" (kW/m^2)
1	21	0.5334	0.007609589	770.797596	
2	33	0.8382	0.011957926	773.7694686	46.60125201
3	45	1.143	0.016306263	797.7749186	46.40977714

4	57	1.4478	0.0206546	731.8397602	38.37562468
5	69	1.7526	0.025002937	593.6967509	29.80720609
6	81	2.0574	0.029351274	504.0551855	20.74602491
7	93	2.3622	0.03369961	401.9343485	
8	105	2.667	0.038047947	325.3268831	
Vdot (CFM)			**13**		
HRR' (kW/m)			**675.1536004**		
Nominal Height	Height	**Height (m)**	z/Q'^(2/3)	T [C]	q" (kW/m^2)
1	21	0.5334	0.00693082	777.1996754	
2	33	0.8382	0.010891289	789.7759148	48.38587894
3	45	1.143	0.014851757	820.2030581	50.87255678
4	57	1.4478	0.018812226	770.5730466	42.29629975
5	69	1.7526	0.022772694	638.1858724	33.31745057
6	81	2.0574	0.026733163	553.7751645	24.86389794
7	93	2.3622	0.030693631	457.7312281	
8	105	2.667	0.0346541	382.0502365	

Appendix L – Gas Burner Background

Gas Burner Design Burner Types

The main benefit of using a gas burner to simulate fire scenarios is the ability to replicate the scenarios reliably. Gas burners can be designed to provide the desired heat flux to test the desired material exactly as one wants. Things that can be varied when testing that can change how the gas burner operates include the flow rate of the burning gas, the heat content of the gas, and the distance between the burner and the material. Getting the right temperature of the burner is very important and can easily be modified by the mass flow rate of the gas and by varying the type of gas used.

For the fire test that our group will be preforming, we will use a porous surface burner. The main benefit of a porous surface burner is that it best replicates the way a real fire behaves. It does this by "leaking" the fire out as opposed to a jet type burner that propels the flame out which gives the flame a velocity that does not replicate how a fire would act in our project.

For this test we will be using a diffusion burner. This means that the fuel, propane for example, is pushed through the burner before it meets the air, this means that no flame can be present until the fuel mixes sufficiently with the air around it because there would be a lack of oxygen. One way to tell what is a diffusion flame is that they generally produce an orange- yellow flame. This is very different from a premixed burner, which mixes the air and fuel inside the burner resulting in a bluish flame right out of the burner. For the most part, porous surface burners will also be diffusion burners, and jet burners will be premixed, although there are a few times where this is not true.

Flame Height Against a Wall

An extensive experimental study was performed by Back et al.[10] shows two popular methods are to videotape the flames or to use thermocouples. Using the 50% visual intermittency criterion for flame height is a standard for the camera, while thermocouple measurements use the 500°C average centerline temperature criterion to determine their flame heights. During that experiment the two different methods matched up well for the most part with only a few tests off by about .09 meters as you can see below.

Test Number	Q (kW)	D (m)	Videotape Flame Height (m)	500°C Flame Height (m)
1	53	0.28	0.79	0.78
2	56	0.70	0.36	0.33
3	68	0.48	0.60	0.51
4	106	0.37	1.00	1.02
5	136	0.48	0.87	0.86
6	204	0.48	1.45	1.45
7	220	0.70	1.20	1.29
8	313	0.57	2.20	2.29
9	523	0.70	--	2.9

Figure 8 - The Flame Heights Produced From a Square Propane Fueled Sand Burner on a Flat Wall

In the experiment Back et al. used several square propane fueled sand burners of different sizes and with different heat release rates to test the flame height against an adjacent gypsum wall.

Heat Flux to a Wall

In the same experiment by Back et al. they determined the centerline temperature, through Equations 1 and 2 below and determined that the peak heat flux for the plume produced occurred at the centerline 15 cm. above the sand burner with the exception of the 300 and 500 kW fires.

$$\Delta T_{CL} = 40.6\, \dot{Q}^{2/3} (Z - Z_o)^{-5/3} \qquad (Z - Z_o) / \dot{Q}^{2/5} > 0.16 \quad (1)$$

$$\Delta T_{CL} = 43.0\, \dot{Q}^{2/3} (Z - Z_o)^{-5/3} \qquad (Z - Z_o) / \dot{Q}^{2/5} > 0.18 \quad (2)$$

They determined that the peak heat flux is independent of the flame shape or aspect ratio and instead is affected by the energy release rate. The peak heat flux then can be expressed as the radiation from a grey emitting flame volume, shown in Equation 3 below. Another way to express the peak heat flux is shown in Equation 4 below.

$$\dot{q}_p'' = E\,(1 - \exp(-kL_m)) \quad (3)$$

$$\dot{q}_p'' = E\,(1 - \exp(-k_\beta \dot{Q}^{1/3})) \quad (4)$$

Figure 2 below shows the maximum heat flux of the wall correlated with the energy release. As you can see, for the majority of the points the aspect ratio is not a big factor.

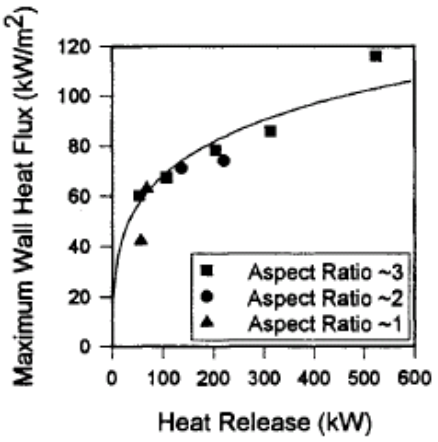

Figure 9 – Lattimer Heat Flux to a Wall

As demonstrated by Brian Lattimer in the SFPE Handbook of Fire Protection Engineering, it is possible to accurately predict the heat transfer from fires to flat walls through the use of empirical formulas. However, these values are highly dependent on the type of fire including the geometry of the surface being heated. In an experiment completed by Back et al propane sand burners are used to calculate the heat transfer from a fire to an adjacent flat wall. During the study, heat fluxes ranged from 50 to 520kW. It was determined that the peak heat flux of these fires were a function of a higher heat release rate which resulted in a thicker boundary layer. By applying the gray-gas radiation theory, it was determined that heat flux with this geometry could be represented with the following equation.[11]

$$q''_{peak} = 200(1 - e^{-.09Q^{\frac{1}{3}}})$$

Peak heat release rates were measured along the centerline in the lower part of the fire. Above the continuous region of the flame, heat fluxes were measured to decrease with distance above the burner. The data obtained by the group supports Lattimer's claim that peak heat flux is a function of heat release rate. The vertical heat flux distribution along the centerline of a rectangular fire shown in Figure 10.

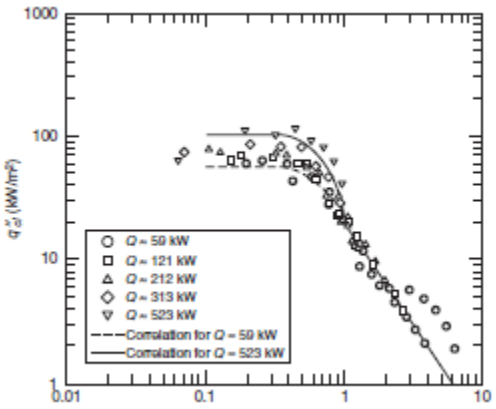

Figure 10 - Lattimer Peak Heat Flux Data[11]

Burner Overview

Geometric Replication of NFPA 285

One challenge in adapting the full scale NFPA 285 calibration parameters to the intermediate scale test is creating an appropriate sized burner. The full scale version has a 78 inch window opening, while the intermediate scale version (which is intended to represent the top of the window opening) is only 48 inches wide, a reduction of 38%. The window burner of the full scale test produces a flame that spans 44 inches, which can be used on the intermediate scale version. If so, the provided calibration information in NFPA 285 can be used and applied to obtain the proper gas flow rates needed. Alternatively, another option is to reduce the burner length proportionally to the width of the intermediate scale test compared to that of the full scale version. This would make the new burner length 27 inches.

Cylindrical Port Burner

A cylindrical port burner would be constructed off a similar framework of the NFPA 285 specified burner. This would allow the ease of connection between testing setups. The cylindrical port burner will use a length of pipe, with a variety of holes drilled into the face. This provides the greatest benefit in flexibility. By varying the size of the ports and their location, it may be possible to fine tune heat flux values much more finitely than the simple slot provided by the NFPA 285 burner. The size of the ports could be variable, which would in turn equate to a higher flow rate of the gas and concurrently heat release rate from that section of the pipe. Additionally varying the ports radial location will change the angle of incident on the wall from that plume. Varying the axial location allows changes to be made along the face of the wall. Figure 9 shows an example cylindrical burner from Jimenez, Finney, and Cohen.[12]

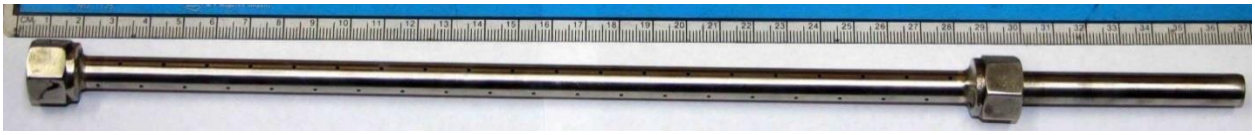

Figure 11 - Sample Cylindrical Port Gas Manifold

This example uses 56 1.16 mm ports, evenly spaced both axially and radially in order to provide a uniform flame. In addition to the ported manifold, the example burner also used a fiberglass sleeve, perforated tube diffuser and ceramic burner tube. Figure 10 shows an example of the flame produced by such a burner.

Figure 12 - Sample Flame of Cylindrical Port Burner

Rectangular Pan Burner

A rectangular pan burner is a popular choice for many fire tests. These burners are able to be closely regulated by controlling the mass flow rate of the gas, which provides consistent and repeatable results. A benefit of these burners over a line burner is that there will be added depth to the flame. This is more realistic for many applications because real fires have a component of depth to them that could affect how it spreads.

Fuel Choice

To determine the fuel we plan to use for our burner, we analyzed the benefits and shortcomings of three different gases. We researched MAPP gas, propane and natural gas while comparing all three with respect to their cost efficiency and flame temperature. To best simulate a real-life fire situation of our experiment, we wanted to identify a gas with a close flame temperature to wood combustion.

MAPP Gas

MAPP gas is one of the fuel source options for the burner. A mixture of methyl acetylene-allene[13], MAPP gas is often used in welding purposed because of its high flame temperature of 2,010°C in air[14]. The main disadvantage to MAPP gas is its expensive price, often much more expensive than propane. Because of this, MAPP gas is often used in small-scale experiments rather than industrial experiments.

Propane

Propane, a product resulting from the processing of petroleum and natural gas, is another option for the fuel source of the burner. One of the benefits of propane is that it includes an ethanethiol, an odorant that is easily detected in the case of a gas leak. As students, this aspect may provide additional safety. Propane also has a flame temperature of 1,967°C in air, which is close to the 1,949°C flame temperature of wood combustion.[14] Because of the similarities in flame temperature between the experiment and real-world situations, propane should be preferred over MAPP gas in our experiment.

Natural Gas

The other option that we considered for our fuel source is natural gas. Natural gas is a fossil fuel which results from the remains of plants and animals from millions of years ago. The primary uses for natural gas is residential and commercial heating as well as transportation.[15] NFPA 285 offers a table, which can be easily used to regulate flow rates in laboratory research. Natural gas also has a flame temperature of 1960°C[14]; nearly identical to wood combustion flame temperature. As result, we recommend using natural gas as we move forward in our testing.

Appendix M – FDS Input File

```
&HEAD CHID='MODEL', TITLE='Sourcefire_MQP'/

&MESH IJK = 30,30,22, XB= 0.00,3.0, 0.00,3.0, 0.00,2.2/
&MESH IJK = 10,30,40, XB= 3.0,4.0, 0.0, 3.0, 0.0,4.0/

&DUMP DT_RESTART=50/
&TIME T_END=1800/

&REAC ID                    = 'METHANE'/

/MATL ID                    = 'CONCRETE'
      SPECIFIC_HEAT                 = 0.88
      CONDUCTIVITY                  = 1.0
      DENSITY               = 2000 /

&SURF ID                    = 'CONCRETE'
      COLOR                         = 'GRAY'
      ADIABATIC             =.TRUE.
      THICKNESS             = .200
      BACKING               = 'EXPOSED'/

&OBST XB= 0.0,0.0, 0.0,3.0, 0.0,2.2, COLOR='GRAY'/BACK WALL
&OBST XB= 3.0,3.2, 0.0,3.0, 0.0,4.0, COLOR='GRAY'/FRONT WALL
&OBST XB= 0.0,3.0, 0.0,0.0, 0.0,2.2, COLOR='INVISIBLE'/SIDE WALL
&OBST XB= 0.0,3.0, 3.0,3.0, 0.0,2.2, COLOR='INVISIBLE'/SIDE WALL
&OBST XB= 0.0,3.0, 0.0,3.0, 2.2,2.2, COLOR='GRAY'/CEILING

&HOLE XB= 2.9,3.3, 0.5,2.5, 0.7,1.5,/WINDOW

&HOLE XB= 1.3,1.7, -0.1,0.1, 0.0,0.4,/VENT
&HOLE XB= 1.3,1.7, 2.9,3.1, 0.0,0.4,/VENT

&VENT MB=ZMAX, SURF_ID='OPEN'/
&VENT MB=XMAX, SURF_ID='OPEN'/
&VENT MB=XMIN, SURF_ID='OPEN'/
&VENT MB=YMAX, SURF_ID='OPEN'/
&VENT MB=YMIN, SURF_ID='OPEN'/

&OBST XB= 1.2,1.8, 1.2,1.8, 0.0,0.8,COLOR='BLACK'/BURNER

&SURF ID='ROOMBURNER', HRRPUA=2511, COLOR='RED',RAMP_Q='ROOM'/
&RAMP ID='ROOM', T=0,F=.76/
&RAMP ID='ROOM', T=600,F=.86/
&RAMP ID='ROOM', T=900,F=.92/
&RAMP ID='ROOM', T=1500,F=1/
```

```
&VENT XB= 1.2,1.8, 1.2,1.8, 0.8,0.8, SURF_ID='ROOMBURNER'/

&OBST XB = 3.3,3.4, .75,2.25, 1.15,1.25, COLOR='BLACK', THICKEN=.TRUE./WINDOW BURNER

&SURF ID='WINDOWBURNER', HRRPUA=2653, COLOR='RED',RAMP_Q='WINDOW'/
&RAMP ID='WINDOW', T=0,F=0/
&RAMP ID='WINDOW', T=300,F=.41/
&RAMP ID='WINDOW', T=600,F=.55/
&RAMP ID='WINDOW', T=900,F=.73/
&RAMP ID='WINDOW', T=1200,F=.86/
&RAMP ID='WINDOW', T=1500,F=1/

&VENT XB= 3.3,3.4, .75,2.25, 1.25,1.25, SURF_ID='WINDOWBURNER', IOR=3/

&SLCF QUANTITY='TEMPERATURE', PBY=1.5/
&SLCF QUANTITY='TEMPERATURE', PBX=3.2/
&SLCF QUANTITY='HRRPUV', PBY=1.5/
&SLCF QUANTITY='HRRPUV', PBX=1.5/
&SLCF QUANTITY='VELOCITY', PBY=1.5/
&SLCF QUANTITY='VOLUME FRACTION', SPEC_ID='OXYGEN', PBY=1.5/

&DEVC ID='TC15', XYZ= 3.0,0.915,1.825, QUANTITY='WALL TEMPERATURE', IOR=-1/
&DEVC ID='TC16', XYZ= 3.0,1.5,1.825, QUANTITY='WALL TEMPERATURE', IOR=-1/
&DEVC ID='TC17', XYZ= 3.0,2.135,1.825, QUANTITY='WALL TEMPERATURE', IOR=-1/

&DEVC ID='TC18', XYZ= 2.29,0.76,1.98, QUANTITY='TEMPERATURE'/
&DEVC ID='TC19', XYZ= 2.29,2.29,1.98, QUANTITY='TEMPERATURE'/
&DEVC ID='TC20', XYZ= 1.5,1.5,1.98, QUANTITY='TEMPERATURE'/
&DEVC ID='TC21', XYZ= 0.76,0.76,1.98, QUANTITY='TEMPERATURE'/
&DEVC ID='TC22', XYZ= 0.76,2.29,1.98, QUANTITY='TEMPERATURE'/

&DEVC ID='TC2', XYZ= 3.25,1.5,1.82, QUANTITY='TEMPERATURE'/
&DEVC ID='TC3', XYZ= 3.25,1.5,2.12, QUANTITY='TEMPERATURE'/
&DEVC ID='TC4', XYZ= 3.25,1.5,2.42, QUANTITY='TEMPERATURE'/
&DEVC ID='TC5', XYZ= 3.25,1.5,2.72, QUANTITY='TEMPERATURE'/
&DEVC ID='TC6', XYZ= 3.25,1.5,3.02, QUANTITY='TEMPERATURE'/
&DEVC ID='TC7', XYZ= 3.25,1.5,3.32, QUANTITY='TEMPERATURE'/

&DEVC ID='C2', XYZ= 3.2,1.5,1.82, QUANTITY='GAUGE HEAT FLUX', IOR=1/
&DEVC ID='C3', XYZ= 3.2,1.5,2.12, QUANTITY='GAUGE HEAT FLUX', IOR=1/
&DEVC ID='C4', XYZ= 3.2,1.5,2.42, QUANTITY='GAUGE HEAT FLUX', IOR=1/

&DEVC ID='SILL_Q', XYZ= 3.1,1.5,1.5, QUANTITY='GAUGE HEAT FLUX', IOR=-3/
&DEVC ID='SILL_Q_L', XYZ= 3.1,0.9,1.5, QUANTITY='GAUGE HEAT FLUX',IOR=-3/
&DEVC ID='SILL_Q_R', XYZ= 3.1,2.1,1.5, QUANTITY='GAUGE HEAT FLUX',IOR=-3/
&DEVC ID='MASS FLOW',QUANTITY='MASS FLOW +', XB=2.9,3.3, 0.5,2.5, 0.7,1.5, IOR=-2/
&DEVC ID='O2', QUANTITY='VOLUME FRACTION', SPEC_ID='OXYGEN', XYZ = 0.5, 1.5, 1.5/
&TAIL /
```

References

[1] "Thermocouple." *What Is a Thermocouple-Types of Thermocouples*. Thermocouple Info, n.d. Web. 29 Apr. 2015. <http://www.thermocoupleinfo.com/>.

[2] "Thin Skin Calorimeter." *Thin Skin Calorimeter - Fire Science Tools*. N.p., n.d. Web. 29 Apr. 2015. <https://sites.google.com/site/srcombexp/home/instrumentation-diagnostics/thin-skin-calorimeter>.

[3] De Ris, J.,and M. Khan, "A Sample Holder for Determining Material Properties," Fire and Materials, 24 (2000) 219-226.

[4] "Schmidt-Boelter." *Heat Flux Specialists*. N.p., n.d. Web. 14 Sept. 2014. <http://www.vatell.com/node/6>.

[5] "Bidirectional Probe - Fire Science Tools." *Bi Directional Probe - Fire Science Tools*. N.p., n.d. Web. 05 Sept. 2014.

[6] *Building Envelope Design Guide - Wall Systems,* Lemieux and Totten, National Institute of Building Sciences, Aug. 2010, Accessed at http://www.wbdg.org/design/env_wall.php#funda

[7] Kingspan Benchmark, Accessed at http://www.kingspanpanels.us/benchmark/products/engineered-facade-systems/metallics/mcm

[8] Parex EIFS Brocheure, Accessed at http://www.parex.com/literature/PEB.pdf

[9] Fundermax Product Details, Accessed at http://www.fundermax.at/max_exterior_%7C_f-quality.en.69.htm

[10] G. Back, C.L. Beyler, P. DiNenno, and P. Tatem, "Wall Incident Heat Flux Distributions Resulting from an Adjacent Fire," in Fire Safety Science—Proceedings of the Fourth International Symposium, International Association of Fire Safety Science, Ottawa, Canada, pp. 241–252 (1994).

[11] Lattimer, Brian Y. "Heat Fluxes from Fires to Surfaces." *SFPE Handbook of Fire Protection Engineering* Third Edition (202): 2-269--272. Web.

[12] Jimenez, Finney, and Cohen. Design and Construction of Gas-Fed Burners for Laboratory Studies of Flame Structure. USDA Forest Service. 2010

[13] "Haz-Map." *Category Details*. N.p., n.d. Web. 18 Oct. 2014. <http://hazmap.nlm.nih.gov/category-details?id=548&table=copytblagents>.

[14] "Flame Temperatures Some Common Gases." *Flame Temperatures Some Common Gases*. N.p., n.d. Web. 18 Oct. 2014.

[15] What Is Natural Gas?" *Alberta Energy:*. N.p., n.d. Web. 15 Oct. 2014. <http://www.energy.alberta.ca/naturalgas/723.asp>.